

KfK 4723
Mai 1990

Corrosion Testing of Selected Packaging Materials for Disposal of High-Level Waste Glass in Rock Salt Formations

**E. Smailos, W. Schwarzkopf, R. Köster, B. Fiehn, G. Halm
Institut für Nukleare Entsorgungstechnik**

Kernforschungszentrum Karlsruhe



Kernforschungszentrum Karlsruhe
Institut für Nukleare Entsorgungstechnik

KfK 4723

**CORROSION TESTING OF SELECTED PACKAGING MATERIALS FOR
DISPOSAL OF HIGH-LEVEL WASTE GLASS IN ROCK SALT FORMATIONS**

E. Smailos, W. Schwarzkopf, R. Köster, B. Fiehn, G. Halm

Work performed under contract FI 1 W-0032 - D with the
Commission of the European Communities as part of its R and D
Programme on "Management and Storage of Radioactive Wastes"

Kernforschungszentrum Karlsruhe GmbH, Karlsruhe

Als Manuskript gedruckt
Für diesen Bericht behalten wir uns alle Rechte vor

Kernforschungszentrum Karlsruhe GmbH
Postfach 3640, 7500 Karlsruhe 1

ISSN 0303-4003

Summary

In previous corrosion studies performed in salt brines, unalloyed steels, Ti 99.8-Pd and Hastelloy C4 have proved to be the most promising materials for long-term resistant packagings to be used in heat-generating waste (vitrified HLW, spent fuel) disposal in rock-salt formations. To characterise the corrosion behaviour of these materials in more detail, further in-depth laboratory-scale and in-situ corrosion studies have been performed in the present study. Besides the above-mentioned materials, also some in-situ investigations of the iron-base materials Ni-Resist D2 and D4, cast iron and Si-cast iron have been carried out in order to complete the results available to date.

The influence has been studied of important parameters on the corrosion of the materials in disposal-relevant media which may be present in normal operation of a rock-salt repository and in certain accident scenarios. These have been: rock salt (H_2O -content: < 0.1 wt.%), rock salt/brines ($MgCl_2$ -rich and $NaCl$ -rich) and an all-brine environment rich in $MgCl_2$ (Q-brine). The parameters investigated have been: corrosion time (3 years at the maximum), temperature ($90^\circ C - 210^\circ C$), H_2S (25-200 mg/l), gamma dose-rate (1 Gy/h-100 Gy/h), and selected characteristics of container manufacturing. For the latter electron beam (EB) welded cast-steel tubes without and with a corrosion protection consisting of Ti 99.8-Pd and Hastelloy C4, respectively, applied by explosion plating have been examined in-situ in heated boreholes.

The results of detailed laboratory and in-situ corrosion experiments are in good agreement; they confirm the finding of previous investigations that unalloyed steels and Ti 99.8-Pd are promising materials for long-term resistant packagings. The three steels (fine-grained steel, low-carbon steel, cast steel) investigated and Ti 99.8-Pd resisted pitting and crevice corrosion as well as stress-corrosion cracking under all test conditions. Gamma dose-rates of 1 Gy/h - 100 Gy/h or H_2S -concentrations in the brines as well as welding and explosion plating did not influence noticeably the corrosion behaviour of the materials. Furthermore, the determined corrosion rates of the steels ($50 \mu m/a - 250 \mu m/a$, depending on the test conditions) are intercomparable and imply technically acceptable corrosion allowances for the thick-walled containers discussed.

For Ti 99.8-Pd no detectable corrosion was observed. By contrast, Hastelloy C4 proved susceptible to pitting and crevice corrosion at gamma dose-rates higher than 1 Gy/h and in the presence of H_2S (25 mg/l) in Q-brine. The materials Ni-Resist D2 and D4, cast iron and Si-cast iron corroded at negligible rates in the in-situ experiments performed in rock salt/limited amounts of $NaCl$ -brine. Nevertheless, these materials must be ruled out as container materials because they have proved to be susceptible to pitting and intergranular corrosion in previous laboratory studies conducted with $MgCl_2$ -rich brine (Q-brine) in excess.

Korrosionsuntersuchungen an ausgewählten Verpackungsmaterialien für die Endlagerung von hochradioaktiven Abfallprodukten in Steinsalzformationen

Zusammenfassung

Bisherige Korrosionsuntersuchungen an einer Reihe von Werkstoffen ergaben, daß unlegierte Stähle, Ti 99.8-Pd und Hastelloy C4 die aussichtsreichsten Materialien für langzeitbeständige Verpackungen zur Endlagerung von wärmeerzeugenden Abfällen (verglaster HAW, abgebrannte Brennelemente) in Steinsalzformationen sind. Zur detaillierteren Charakterisierung ihres Korrosionsverhaltens wurden in der vorliegenden Arbeit weitergehende Labor- und in situ-Korrosionsuntersuchungen durchgeführt. Neben Untersuchungen an den oben genannten Materialien wurden auch einige in situ-Experimente an den Eisenbasiswerkstoffen Ni-Resist D2 und D4, Sphäroguß und Si-Guß durchgeführt, um die bisher vorliegenden Ergebnisse zu vervollständigen.

Es wurde der Einfluß wichtiger Parameter auf die Korrosion der Werkstoffe in endlagerrelevanten Medien untersucht, die bei bestimmungsgemäßem Betrieb des Endlagers oder bei bestimmten Störfällen auftreten können. Diese waren: Steinsalz (H_2O -Gehalt: $< 0,1$ Gew. %), Steinsalz/Salzlösungen ($MgCl_2$ - und $NaCl$ -reich) und die $MgCl_2$ -reiche Q-Lösung. Folgende Parameter wurden untersucht: Korrosionszeit (maximal 3 Jahre), Temperatur ($90^\circ C$ - $210^\circ C$), H_2S (25 - 200 mg/l) und Gamma Dosisleistung (1 Gy/h-100 Gy/h). Darüberhinaus wurde der Einfluß ausgewählter Herstellungsbedingungen für Behälter auf die Korrosion von Stahl, Ti 99.8-Pd und Hastelloy C4 untersucht. Dazu wurden elektronenstrahlgeschweißte Stahlgußrohre ohne und mit sprengplattiertem Korrosionsschutz aus Ti 99.8-Pd bzw. Hastelloy C4 in beheizten Bohrlöchern untersucht.

Die Ergebnisse der Labor- und in situ-Korrosionsuntersuchungen zeigten gute Übereinstimmung; sie bestätigten die Ergebnisse früherer Untersuchungen, daß unlegierte Stähle und Ti 99.8-Pd aussichtsreiche Materialien für langzeitbeständige Verpackungen sind. Die drei untersuchten Stähle (Feinkornbaustahl, Weichstahl und Stahlguß) und Ti 99.8-Pd waren bei allen Prüfbedingungen beständig gegenüber Loch- und Spaltkorrosion sowie Spannungsrißkorrosion. Gamma Dosisleistungen von 1 Gy/h-100 Gy/h oder H_2S -Konzentrationen in den Lösungen zwischen 25 mg/l und 200 mg/l hatten keinen signifikanten Einfluß auf die Korrosion der obigen Werkstoffe. Das gleiche gilt auch für das Schweißen und Sprengplattieren. Darüberhinaus waren die ermittelten Korrosionsraten der Stähle in allen Prüfmedien untereinander vergleichbar und die Werte ($50 \mu m/a$ - $250 \mu m/a$ je nach Prüfbedingungen) führen zu akzeptablen Korrosionszuschlägen für die diskutierte dickwandige Verpackung.

Für Ti 99.8-Pd war unter den Prüfbedingungen kein meßbarer Korrosionsangriff festzustellen. Bei Hastelloy C4 hingegen trat bei Gamma-Dosisleistungen höher als 1 Gy/h und in Gegenwart von H_2S (25 mg/l) in der Q-Lösung Loch- und Spaltkorrosion auf. Die Werkstoffe Ni-Resist D2 und D4, Sphäroguß und Si-Guß korrodierten bei den in situ-Experimenten in Steinsalz plus kleinen Mengen $NaCl$ -Lösung mit geringer Abtragsrate. Trotz dieses Ergebnisses eignen sie sich nicht als Werkstoff für langzeitbeständige Behälter, da sie in früheren Laboruntersuchungen, in denen $MgCl_2$ -reiche Lösung (Q-Lösung) im Überschuß verwendet wurde, eine hohe Empfindlichkeit gegenüber Loch- und interkristalliner Korrosion gezeigt haben.

Table of contents

	Page
	Summary
1.	Introduction 1
2.	Laboratory-scale corrosion studies 2
2.1	Materials investigated and types of specimen 2
2.2	Test conditions 3
2.3	Experimental procedure 5
2.4	Results and discussion 6
2.4.1	Corrosion studies without irradiation 6
2.4.2	Corrosion studies with gamma irradiation 7
2.4.3	Influence of H ₂ S on corrosion 9
3.	In-situ corrosion studies in the Asse salt mine 10
3.1	Investigations in rock salt at rock temperature 11
3.2	Investigations in rock salt/limited amounts of brine at HLW design temperature 12
3.2.1	Experimental set-up and test conditions 13
3.2.2	Results and discussion 14
3.3	Testing of welded tubes in rock salt/brine at HLW design temperature 15
3.3.1	Test conditions and experimental set-up 16
3.3.2	Post-test investigation of the tubes 17
3.3.3	Results and discussion 17
3.4	Testing at elevated temperature and in an elevated gamma radiation field 18
4.	Conclusions 20
5.	Literature 22

1. Introduction

Radioactive waste disposal in deep rock-salt formations is based on the concept of isolating the radionuclides from the biosphere by combining geological with engineered barriers. One element of this multi-barrier concept is the waste packaging. Accordingly, within the Research Programme of the European Communities studies are being performed at KfK which aim at qualifying materials for a long-term resistant packaging to be used in the disposal of high-level waste (HLW) canisters. This packaging is to serve as a barrier against radionuclide mobilisation from the HLW forms during the high temperature phase ($> 100^{\circ}\text{C}$) in the disposal area which lasts a few 10^2 years. To achieve this goal, the packaging material must meet the requirements of sufficiently long-term corrosion resistance in rock salt and in salt brines. Salt brines in the disposal area may originate from the thermal migration of brine inclusions in rock salt and have to be considered in accident scenarios, such as brine inflow through an anhydride layer..

Previous corrosion studies performed at KfK on a large number of materials [e.g. 1,2,3] in an all-liquid brine environment have shown that unalloyed steels, Ti 99.8-Pd, and Hastelloy C4 are the most promising materials for HLW packagings. Consequently, further laboratory-scale and in-situ corrosion studies were performed on these materials within the framework of the 3rd European Communities container programme (1986-1989) in order to characterise their corrosion behaviour in more detail. The studies concerned the determination of the corrosion behaviour of the materials in disposal-relevant corrosion media (rock salt/brines two-phase media and one-phase brine) under the influence of temperature, gamma dose-rate, H_2S -content in brines and selected characteristics of container manufacturing. In addition, some studies were carried out on the iron-base materials cast iron, Ni-Resists and Si-cast iron in order to complete the results available up to now.

The investigations focussed on the unalloyed steels undergoing active corrosion in salt brines because only general corrosion has been observed until now so that their long-term corrosion behaviour can be calculated more easily than that of Ti 99.8-Pd and Hastelloy C4 which undergo passive corrosion.

An essential aspect of the laboratory-scale corrosion studies was the investigation of the influence exerted by gamma radiation from HLW on the corrosion behaviour of the steels and Hastelloy C4. Such investigations are important because

the radiolytic products formed by the effect of radiation on salt brines, e.g. H_2O_2 , ClO^- , ClO_3^- [4], might influence the corrosion process. Preliminary studies [5] performed at $90^\circ C$ and at a gamma dose-rate of 1000 Gy/h ($10^5 rad/h$) based on the present design of a 5 mm thin-walled HLW canister have shown much higher corrosion rates for unalloyed steels and Hastelloy C4 than in the absence of radiation. For Ti 99.8-Pd no influence on corrosion was observed at this dose rate. For a packaging acting as a barrier in the repository a wall thickness of about 100 mm is needed to guarantee the mechanical stability against the rock pressure of 36 ± 5 MPa [6] at 1000 m depth in the disposal area. In this case, the expected dose rate on the surface of the HLW packaging will be lower than 10 Gy/h. For this reason, experiments were performed at realistic dose rates of 1 Gy/h and 10 Gy/h as well as at the higher dose rate of 100 Gy/h in order to have more severe conditions.

2. Laboratory-scale corrosion studies

2.1 Materials investigated and types of specimen

Three preselected unalloyed steels, namely fine-grained steel, low-carbon steel and cast steel, and the Ni-Cr-Mo alloy Hastelloy C4 were investigated. The materials were tested in rock salt/brines two-phase corrosion media as well as in an all-liquid brine environment which may be present during normal operation of the repository or in certain accident scenarios (see Section 2.2).

The chemical compositions of the materials are given in Tab. 1. Compared with the fine-grained steel, the low-carbon steel has a lower content of C, Si and Mn; cast steel is the equivalent casting quality of fine-grained steel. Fine-grained steel, low-carbon steel and Hastelloy C4 were examined as hot-rolled and normalized sheet metals, whereas cast steel was tested in the as cast condition.

All materials were examined for general and pitting corrosion. In case of fine-grained steel and Hastelloy C4 the susceptibility to crevice and stress-corrosion cracking was studied in addition. Furthermore, the influence was investigated of potential container sealing techniques as Tungsten Inert Gas Welding (TIG) and Electron Beam Welding (EB) on the corrosion of fine-grained steel and Hastelloy C4.

To determine general corrosion, non-welded plain specimens of 50 mm x 20 mm x 4 mm and 40 mm x 40 mm x 10 mm (cast steel), respectively, were used. In the examinations relating to stress-corrosion cracking U-bent specimens (80 mm x 15 mm x 4 mm) with 18 mm leg spacing were used. For the investigations into the influence of welding on the corrosion of fine-grained steel and Hastelloy C4, some of the plain and U-bent specimens were provided with TIG and EB welds. The crevice corrosion specimens consisted of two plain specimens connected by a screw of the same material. All specimen types were also evaluated for their susceptibility to pitting corrosion.

2.2 Test conditions

Two corrosion scenarios were considered:

- Intrusion of large amounts of an $MgCl_2$ -rich brine (Q-brine) into the HLW boreholes during the initial phase of disposal, i.e., while the annular gap between the HLW packaging and the borehole wall is still open. In this case, an all-brine environment is present. $MgCl_2$ -rich brines are present in far-distant areas in the repository and might inflow into the boreholes in accident scenarios
- Intrusion of smaller amounts of salt brines ($MgCl_2$ -rich and NaCl-rich) into the HLW boreholes at a later time of disposal, i.e., after the rock salt has already come into contact with the HLW packaging due to the thermally induced borehole convergence. In this case, a two-phase corrosion medium consisting of rock salt/brine is present. NaCl-rich brines, which occur in limited amounts as inclusions in rock salt may undergo thermal migration from the immediate zone of the boreholes to the containers during normal operation of the repository.

The composition of the brines used and the values measured of the pH and saturated O_2 -concentrations have been indicated in Tab. 2. The Q-brine was prepared by dissolving NaCl, KCl, $MgSO_4 \cdot 7H_2O$ and $MgCl_2 \cdot 6H_2O$ in demineralised water. The NaCl-rich brine was prepared by dissolving rock salt from the Asse salt mine in demineralised H_2O . The most important constituents of Asse rock salt (g/l) are:

Na⁺:357.3; K⁺:5.6; Ca²⁺:21.7; Mg²⁺:2.0; Cl⁻:563.4; SO₄²⁻:49.9.

In order to simulate the conditions of an intrusion of large amounts of brine into the HLW boreholes a specimen surface to brine volume ratio (S/V) of 1 cm²/5 ml was selected. This resembles approximately the case of total filling with brine the gap existing between the HLW packaging and the borehole wall. To simulate the case that rock salt plus smaller amounts of brine are present as corrosion media, an S/V ratio of 1 cm²/1 ml and 10 wt.% H₂O-content of rock salt were chosen. Immersion tests with even smaller amounts of brine are not feasible.

The test conditions for the steels and Hastelloy C4 in Asse rock-salt/Asse rock-salt brine, Asse rock-salt/Q-brine and Q-brine are given in Tab. 3. The following investigations were performed:

- Comparative corrosion studies on the three steels with a view to selecting a reference steel for further investigations. These included testing of the steels in the rock salt/brines two-phase corrosion media at 90°C and 170°C without irradiation as well as in the Q-brine at realistic gamma dose-rates of 1 Gy/h and 10 Gy/h for the thick-walled container discussed. On the basis of these results and considering the aspects of strength and weldability, fine-grained steel was selected as the reference steel.
- Additional investigations of fine-grained steel were carried out in rock salt/salt brines at gamma dose-rates of 1 Gy/h and 10 Gy/h at 90°C as well as in the all-liquid Q-brine environment at a higher dose rate of 100 Gy/h in order to have more severe conditions. Furthermore, the influence was studied of different concentrations of the thermally released salt impurity H₂S on the corrosion of this steel in Q-brine. For this, H₂S was added to Q-brine as Na₂Sx9H₂O at the concentrations 25 mg/l, 100 mg/l and 200 mg/l. These values correspond to the amounts released from 10 cm, 20 cm and 40 cm thick ring-shaped salt elements around an HLW borehole. For comparison, also investigations were performed in H₂S-free brine.
- Investigations into the influence of gamma dose-rate (1 Gy/h-100 Gy/h) and H₂S (25 mg/l) on Hastelloy C4 corrosion in Q-brine.

The maximum duration of all tests was one year. The test temperatures of 150°C-170°C roughly correspond to the maximum surface temperature of the HLW containers according to the German borehole concept. The experiments performed at 90°C served as a direct comparison with the results of previous investigations

made at the same temperature in Q-brine without irradiation and with irradiation of 1000 Gy/h [5]. Investigations under gamma irradiation at the maximum HLW disposal temperature ($\leq 200^{\circ}\text{C}$) according to the German borehole concept are under way.

2.3 Experimental procedure

For the experiment without irradiation two different setups were used. The experiments at 90°C were performed at atmospheric pressure in cylindrical glass vessels of 250 ml volume. In these vessels specimens cleaned with alcohol in an ultrasonic bath were immersed into Q-brine or embedded into loose Asse rock-salt of ≤ 3 mm grain size. After precompaction of the rock salt with a metal die the prefabricated Asse rock-salt brine and Q-brine were added and the glass vessels tightly sealed.

For the experiments at 150°C and 170°C (without irradiation) stainless steel pressure vessels provided with corrosion resistant insert vessels made of PTFE ($V = 250$ ml) were used in order to avoid evaporation of the brines (boiling point: 115°C). The experiments were carried out at equilibrium pressure of 0.4-0.55 MPa. In these vessels the specimens were immersed into Q-brine or embedded into Asse rock-salt as in the experiments at 90°C , and the salt brines were subsequently added. After the glass vessels and the pressure vessels had been closed, they were stored in heating chambers at 90°C and 170°C , respectively.

The corrosion experiments under gamma irradiation were performed in the spent fuel element storage pool of KFA Jülich. The radiation source were spent fuel elements of different degrees of burnup with a gamma-energy spectrum similar to that of 10 years old vitrified HLWC [7] (Fig. 1). The experimental set-up is shown schematically in Fig. 2. The material specimens and the corrosion media (brine and rock salt with brine additions) were contained in tubular vessels made of Duran glass. The glass vessels were placed in a circular configuration in heated cylindrical stainless steel containers (irradiation containers).

For irradiation the containers were positioned on the bottom of the 6 m deep water-filled spent fuel element storage pool. The specimens and corrosion media were heated to the 90°C test temperature using cartridge type heaters. Radiolytic gases and hydrogen generated by corrosion during the experiments were discharged into the atmosphere by purification with helium.

After removal from the corrosion media, the specimens were cleaned and examined for general and local corrosion as well as for stress-corrosion cracking by gravimetry, measurement of pitting depths, surface profilometry, and metallography.

2.4 Results and discussion

2.4.1 Corrosion studies without irradiation

In both two-phase testing media consisting of Asse rock-salt/Asse rock-salt brine and Asse rock-salt/Q-brine the three unalloyed steels investigated exhibited a comparable corrosion behaviour. The specimens suffered mainly from uniform corrosion attack although minor specimen zones of non-uniform corrosion attacks with shallow pit formation were also observed. While the temperature rose from 90°C to 170°C the average general corrosion and the depth of shallow pits likewise increased. The non-uniform corrosion on the steels is attribute to inhomogeneities in their compositions. The micrographs (Figs. 3 and 4) of fine-grained steel show in a way which is representative of all steels that non-uniform corrosion attack takes place in both testing media at 90°C and 170°C. Pitting and crevice corrosion in the sense of an active-passive corrosion element or stress-corrosion cracking were not observed. Furthermore, TIG welding or EB welding did not exert a noticeable influence on the corrosion behaviour of the steels.

Figures 5 and 6 show the time-temperature behaviour of the general corrosion rates of the steels in the test media. The values are mean values of 3 to 6 comparative specimens. The ranges of corrosion rates represented as bars show the standard deviations of the measured values. It is evident from the standard deviations that the general corrosion rates of the comparative specimens are often subjected to great variations with respect to each other. This is attributed to the irregular distribution of the salt grit. The cause is deemed to be the statistical differences in pore distribution in the salt. This means that specimens in the zone of the salt grit with a higher porosity were exposed to a larger brine volume than specimens kept in zones of higher density salt occurrence.

In rock salt/rock-salt brine no dependence was found of the general corrosion rates of steels on the test duration. The average corrosion rates scattered from 5 $\mu\text{m/a}$ to 20 $\mu\text{m/a}$ at 90°C and from 25 $\mu\text{m/a}$ to 40 $\mu\text{m/a}$ at 170°C, respectively. Also in rock salt/Q-brine time-independent corrosion rates (50-60 $\mu\text{m/a}$ at 90°C and 100-130 $\mu\text{m/a}$ at 170°C) established for all steels after extended test durations. In

general, it can be stated that the general corrosion rates of the steels in both media and at both temperatures differ from each other by only about 30% at the maximum, except for the corrosion rate of cast steel in rock salt/Q-brine at 170°C. In this case, the corrosion rate (230 $\mu\text{m/a}$) was higher by a factor of 1.5-2.5 compared with the two hot-rolled steels. By increase in temperature from 90°C to 170°C, the general corrosion rates rose by a factor of approximately 2. Only for cast steel in rock salt/Q-brine an increase in the corrosion rate by a factor of approximately 5 was observed in that temperature range.

The metallographic examinations of steel specimens exposed to rock salt/rock-salt brine have shown maximum penetration rates of shallow pits of 30-40 $\mu\text{m/a}$ at 90°C and of 120 $\mu\text{m/a}$ -150 $\mu\text{m/a}$ at 170°C which are higher by a factor of 2-4 than the average general corrosion rates. Penetration rates of this size imply acceptable corrosion allowances for a thick-walled packaging. In rock salt/Q-brine the values of the maximum penetration rates of shallow pits were only slightly higher than the general corrosion rates.

If one compares the maximum of penetration rates of shallow pit formation of the steels in both testing media, the values found for Asse rock-salt/Q-brine are higher by approximately the factor of 1.5 to 2 than in Asse rock-salt/Asse rock-salt brine. This is attributed to the lower pH of the Q-brine (pH 90°C = 3.6) compared with the Asse rock-salt brine (pH 90°C = 6). At pH values less than 4 acid-induced corrosion actually occurs. The accelerating effect on the corrosion of steels exerted by Mg^{2+} in rock salt compared with Na^{+} is reported in [8], too.

2.4.2 Corrosion studies with gamma irradiation

The time dependence of the general corrosion rates of the steels in the various corrosion media (two-phase media, all-liquid medium) at 90°C and gamma dose rates of 1 Gy/h to 100 Gy/h is plotted in Figs. 7-9. For comparison, also the values determined without irradiation and at 1000 Gy/h [5], respectively, have been entered. All values are average values of three to six specimens.

In Q-brine (Fig. 7) and at a dose rate of 1000 Gy/h which is to be expected to occur on the surface of a 5 mm thin-walled HLW canister, the corrosion rates of fine-grained steel (460 $\mu\text{m/a}$) and cast steel (660 $\mu\text{m/a}$) are higher by about the factor of 15 than the values without irradiation. At realistic dose rates of 1 Gy/h-10 Gy/h for the thick-walled packaging discussed here as well as at the higher dose rate of

100 Gy/h the final corrosion rates of the fine-grained steel are only about 20 $\mu\text{m/a}$ -35 $\mu\text{m/a}$ and thus close to the value obtained in the absence of irradiation (30 $\mu\text{m/a}$). This is in good agreement with the results reported by Westerman et al [8]. In the case of cast steel and low-carbon steel the final corrosion rates at 1 Gy/h and 10 Gy/h of about 20 $\mu\text{m/a}$ -30 $\mu\text{m/a}$ are lower than the values without irradiation (40 $\mu\text{m/a}$ -80 $\mu\text{m/a}$). This effect might be due to the formation of denser corrosion inhibiting Fe_3O_4 layers under irradiation which were observed in the metallographic examinations. The existence of Fe_3O_4 has been proved in the X-ray diffraction analysis of corrosion layers.

In the two-phase corrosion media rock salt/brines (Figs.8 and 9) the dose rates of 1 Gy/h and 10 Gy/h do not influence noticeably the corrosion rate of fine-grained steel, as is the case in the single-phase Q-brine. The final corrosion rate of 30 $\mu\text{m/a}$ of this steel in Asse rock salt/Q-brine is very close to the value in Q-brine. In Asse rock-salt/Asse rock-salt brine under irradiation the steel corrodes after 1 year at a lower rate (10 $\mu\text{m/a}$) than in the Q-brine.

The metallographic examinations and the surface profiles of corroded specimens exhibited a similar corrosion behaviour of the steels under irradiation (1 Gy/h-100 Gy/h) in all test media. As in the absence of irradiation, the corrosion attack was mainly uniform, but specimen zones with non-uniform corrosion attacks were identified, too. This non-uniform corrosion is attributed to inhomogeneities in the composition of steels. However, the measured maximum rates of penetration in such deeper corrosion zones attained only 50 $\mu\text{m/a}$ -60 $\mu\text{m/a}$ and were roughly identical in all media. These values are very close to those obtained without irradiation and imply a technically acceptable corrosion allowance for a long-term HLW packaging. Moreover, the steels were resistant to pitting and crevice corrosion and to stress-corrosion cracking in all test media. Welding did not exert a noticeable influence on their corrosion behaviour. Figure 10 shows by way of example optical micrographs of fine-grained steel after 1 year exposure in the three media at 90°C and 10 Gy/h.

The results of investigations into general and local corrosion of Hastelloy C4 in Q-brine at 90°C and with dose rates of 1 Gy/h-100 Gy/h have been compiled in Tab. 4. For comparison, also the results of the previous investigations carried out both without irradiation and with 1000 Gy/h have been entered. At dose rates between 1 Gy/h and 100 Gy/h the maximum corrosion rates of 0.4 $\mu\text{m/a}$ are low and roughly correspond to the value obtained in the absence of irradiation.

The dose rate in this range did not noticeably influence the corrosion rate. Moreover, this material remained resistant to stress-corrosion cracking and local corrosion even after 12 months exposure to 1 Gy/h. Also when exposed to 10 Gy/h and 100 Gy/h, Hastelloy C4 proved to be resistant to stress-corrosion cracking; but at these dose rates pitting and crevice corrosion of 20 $\mu\text{m}/\text{a}$ at the maximum was detected. However, the penetration rate remained unchanged during the whole testing period of 12 months. At the dose rate of 1000 Gy/h strong pitting and crevice corrosion occurred as already indicated in previous publications [5], the maximum penetration rate being about 1 mm/a. Figure 11 shows characteristic optical micrographs of Hastelloy C4 after 12 months immersion in Q-brine (90°C) and exposure to 1 Gy/h (uniform corrosion) and 10 Gy/h (pitting corrosion of about 20 $\mu\text{m}/\text{a}$).

2.4.3 Influence of H₂S on corrosion

The time dependence of the general corrosion of fine-grained steel at 170°C in Q-brine without and with H₂S added (25 mg/l, 100 mg/l and 200 mg/l) has been indicated in Fig. 12 as integral corrosion rate. All values are averages of two comparative specimens. The ranges of corrosion rates marked as bars show the standard deviations of the measured values.

After a short period of immersion (40 days) the steel exposed to the salt brine with the highest H₂S concentration (200 mg/l) exhibits the lowest corrosion rate (380 $\mu\text{m}/\text{a}$). This effect is probably attributable to the dense (Fe, Mg)(OH)₂ corrosion layer which has developed and which, obviously, acts as a corrosion inhibitor. After extended periods of immersion the corrosion rates in the brines with the lower H₂S concentrations (25 mg/l and 100 mg/l) decrease faster and approach the values in the salt brine with the higher H₂S concentration because higher-density corrosion inhibiting layers area also formed. Finally, after immersion of about 8 months, corrosion rates between about 240 $\mu\text{m}/\text{a}$ and 300 $\mu\text{m}/\text{a}$, establish in all salt brines, with and without H₂S. A extension of the immersion period to 325 days has no further noticeable influence on the corrosion rates of steel.

Generally, it can be stated that H₂S concentrations in Q-brine between 25 mg/l and 200 mg/l have no significant influence on the corrosion rate of the fine-grained steel.

Examinations of corroded steel specimens by surface profilometry and metallography confirm that H₂S concentrations in the Q-brine between 25 mg/l and 200 mg/l do not significantly influence the corrosion behaviour of fine-grained steel. Both in the H₂S free and in the H₂S containing salt brines the steel underwent non-uniform corrosion with approximately the same depth of attack. Non-uniform corrosion attack is attributed to inhomogeneities in the structure and in the composition of the steel, as already discussed. As a matter of fact, the maximum rates of penetration of deeper corrosion zones were only slightly higher than the integral corrosion rates calculated from the mass losses. Pitting corrosion in the sense of an active-passive corrosion element was not observed. The optical micrographs (Fig. 13) of two fine-grained steel specimens show the non-uniform corrosion attack after 325 days in the pure Q-brine and in the 200 mg H₂/l doped Q-brine at 170°C, respectively.

The results of corrosion for Hastelloy C4 in Q-brine, without and with H₂S (25 mg/l) at 150°C, have been compiled in Tab. 5. In the H₂S free solution the material exhibited a very low general corrosion rate of less than 1 µm/a and was resistant to pitting corrosion. Also in the H₂S containing brine the general corrosion rate of the material of 4 µm/a was low; however, in that medium pitting corrosion of 2.3 mm at the maximum occurred after an extended period of immersion (12 months). This local attack started at the edges of cut and propagated to the specimen surface. Besides, crevice corrosion occurred in both salt brines below the PTFE threads by which the specimens had been suspended whereby the attack was more pronounced in the H₂S containing brine. This means that the resistance to corrosion of Hastelloy C4 is markedly reduced by the addition of H₂S to the Q-brine.

3. In-situ corrosion studies in the Asse salt mine

Materials found promising for a long-term resistant packaging in laboratory-scale corrosion studies are being tested additionally under simulated HLW disposal conditions in the Asse salt mine (in-situ experiments). In the in-situ experiments the integral effect can be determined which is exerted by conditions expected in an HLW repository on the corrosion behaviour of the materials. Furthermore, various accident conditions are being simulated in these experiments, e.g. by variations in the composition and amount of attacking salt brines. An important aspect of the in-situ corrosion studies is the investigation of the influence of selected characteristics of container manufacturing on the corrosion behaviour of

promising container materials. For this, two selected container concepts are being examined: steel containers without corrosion protection and those with corrosion protection made of Ti 99.8-Pd and Hastelloy C4, respectively.

In the present work extensive corrosion studies were performed on six selected iron-base materials, Ti 99.8-Pd and Hastelloy C4. The following investigations were carried out:

- Investigations of metal sheets of the materials indicated above in rock salt at rock temperature (32°C) as a reference experiment.
- Investigations of metal sheets under normal operating conditions (HLW design temperature, gamma radiation field, limited amounts of brine thermally released into the boreholes) of a repository. In these experiments, which were performed within the framework of the German/US Brine Migration Test [9], the applied gamma dose-rate ($3 \times 10^2 \text{ Gy/h}$) was about one order of magnitude higher than the value to be expected on the surface of the thick-walled HLW packaging discussed here.
- Testing of cast steel tubes without and with corrosion protection made of Ti 99.8-Pd and Hastelloy C4, respectively, at HLW design temperature under simulating accident conditions with intrusion of larger amounts of brine into the boreholes.

Besides the experiments mentioned above, metal sheets of different materials (steels, Ti 99.8-Pd, Hastelloy C4 etc.) were stored in boreholes in order to study their corrosion behaviour at elevated temperature (250°C) in a gamma radiation field ($5 \times 10^3 \text{ Gy/h}$). These experiments are being performed within the framework of the HLW test disposal [10] which will start in 1990.

3.1 Investigations in rock salt at rock temperature

In a reference experiment five Fe-base materials (fine-grained steel, nodular cast iron, Ni-Resists D2 and D4, Si-cast iron), Hastelloy C4, and Ti 99.8-Pd were investigated in loose rock salt for three years at 32°C rock temperature. For this, specimens consisting of the materials above were stored in small boreholes (50 mm diameter, 200 mm length) at the 775 m level of the Asse salt mine and covered with

salt grit. The composition of the materials investigated is evident from Tab. 1. The rock salt had the following average composition (in wt.%):

Na⁺: 38.3; K⁺: 0.33; Ca²⁺: 0.17; Mg²⁺: 0.16;
Cl⁻: 58.02; SO₄²⁻: 2.47; H₂O: 0.1.

For nodular cast iron, Ni-Resists, and Si-cast iron only the parent material was studied. For the most promising HLW packaging materials fine-grained steel, Ti 99.8-Pd and Hastelloy C4, the influence of welding on the corrosion behaviour was also studied with a view to container welding in a later application. For this purpose, specimens were examined with a TIG (Tungsten Inert Gas) weld beam applied.

All material specimens were examined for their resistance to general corrosion (weight change) and local corrosion with an electronic depth gauge as well as by surface profilometry and metallography. Plane specimens with the following dimensions were used: Ti 99.8-Pd, Hastelloy C4, fine-grained steel and Si-cast iron 40 mm x 20 mm x 4-5 mm; rest materials 50 mm x 10 mm x 10 mm.

The integral weight losses of the specimens determined by gravimetry and the corrosion rates calculated from them have been entered in Tab. 6. No measurable corrosion attack was observed on Ti 99.8-Pd, Hastelloy C4, Ni-Resist D4, and Si-cast iron. Also for the materials, fine-grained steel, nodular cast-iron and Ni-Resist D2 the corrosion rates of 1 µm/a at the maximum were low. The surface profiles and the metallographic examinations of the specimens in the as-received and welded conditions did not provide indications of local corrosion.

3.2 Investigations in rock salt/limited amounts of brine at HLW design temperature

The experiments were performed within the framework of the German/US Brine Migration Test in the Asse Salt Mine [9] under conditions prevailing during normal operation of a repository (see Section 3.2.1). In these experiments the same materials (Fe-base materials, Ti 99.8-Pd, Hastelloy C4) were tested as in the investigations in Asse rock-salt (Tab. 1), except for Ni-Resist D2, which was replaced by cast steel. Unwelded and TIG welded specimens, as described in Section 3.1, were examined for general corrosion and local corrosion. In addition, some of the Hastelloy C4 specimens were subjected to thermal treatment (maximum temperature 1100°C) either before or after welding in order to test the suitability of Hastelloy

C4 as a container material for direct filling of HLW glass. This simulated loading of the bottom and lid welds of containers in practical application. The thermal treatment of the specimens was described in an earlier publication [11].

3.2.1 Experimental set-up and test conditions

The material specimens to be investigated were stored in four heated, cased boreholes (test sites 1-4). In two of them (test sites 3 and 4) Co-60 sources had been installed. The casing material was a refractory steel with Inconel 600 clad as a corrosion protection. The longitudinal section of one of these boreholes is shown in Fig. 14. The approximately 5 cm wide annular space between the casing and the borehole wall was filled with Al_2O_3 spheres in the bottom part of the borehole in order to prevent the salt from contacting the casing and, on the other hand, maintain the porosity of the annular space for measurement purposes. In the test sites 2 and 4 a gas flow (N_2) was passed through the annular space over the whole test duration, and in the test sites 1 and 3 only at the end of the test. This gas flow carried to the cooling trap the water released by migration into the borehole. By these conditions for the tests the initial phase of disposal was simulated, i.e., the maximum period of three years [12] until closure of the annular gap between the HLW package and the borehole wall. A detailed description of the test set-up is given in [13].

The specimens were located at the borehole wall. The position of the specimens and the corrosion conditions in the borehole are shown in Fig. 14. The maximum temperature of 210°C at the borehole wall conforming to the German disposal concept was set with a heater. During the experiments a vertical temperature profile developed at the borehole wall so that the specimens were exposed to three temperatures: 120°C, 150°C and 210°C. The test temperatures for the individual materials are given in Tab. 7. The maximum gamma dose-rate was 3×10^2 Gy/h and the calculated maximum rock pressure was 28 MPa. The maximum testing period for the materials was 900 days.

It can be noticed that under the selected conditions the brine migrating into the boreholes evaporated so that the specimens were exposed to a steam atmosphere with salt constituents. Besides, gases emanating from the rock salt participated in the corrosion process in addition to gaseous products generated during corrosion of the materials and radiolysis of the brine. The measured values of the volumes and compositions of the brine and gas as well as the temperature profile

and the pressure build-up shown in Fig. 14 are maximum and minimum values applicable to all four boreholes. They were determined by the Institut für Tieflagerung, Braunschweig. Detailed information about the development versus time of the measured values is given in [13] which includes also information about the distribution of the specimens in the boreholes.

3.2.2 Results and discussion

The materials tested corroded at extremely low rates under the in-situ testing conditions, both in the presence and in the absence of gamma radiation. No noticeable influence has been observed of TIG welding or thermal treatment of Hastelloy C4 on the corrosion behaviour of the materials. The weight losses of the unwelded specimens determined by gravimetry and the corrosion rates calculated from them have been entered in Tab. 7. Some specimens did not lend themselves to gravimetric evaluation because they had been damaged mechanically in the course of retrieval. These specimens were used for local corrosion examinations. It is apparent from Tab. 7 that the corrosion rates of all materials not exposed to irradiation are less than $2 \mu\text{m/a}$ and that, except for fine-grained steel, gamma radiation of $3 \times 10^2 \text{ Gy/h}$ has not resulted in an increase in these values.

The low corrosion rates of the materials can be explained by the fact that only 140 ml brine at the maximum had flown into the boreholes by migration which spread over the large surface of about 71 m^2 of the inserts (casing, Al_2O_3 spheres, etc.). Therefore, only a very low amount of brine was available for the corrosion attack of the material specimens with a maximum surface of 250 cm^2 .

The higher corrosion rate determined for fine-grained steel exposed to irradiation (about $14 \mu\text{m/a}$) is probably not caused by the effect of radiation. This assumption relies on the finding that for the similar material cast steel there was no difference in the corrosion rates with and without gamma radiation. The increase in the corrosion rate is probably attributable to the fact that after the heater had been shut down because of plugging of a tube it was not possible to condense more than about half of approximately 1600 ml of inflowing brine. Thus, these specimens suffered from corrosion attack by non-condensed brine for an additional period of about 12 months (i.e., the time interval between shut-down of the heater and specimen retrieval) at a mean temperature of about 70°C .

The metallographic examination of the specimens has shown that, with the exception of fine-grained steel exposed to irradiation, all the other materials undergo uniform corrosion under the in-situ conditions. Figures 15 and 16 show by way of example micrographs of Ti 99.8-Pd, Hastelloy C4 and fine-grained steel before and after storage: In case of fine-grained steel a non-uniform corrosion attack with a maximum penetration of about 25 $\mu\text{m/a}$ was observed which is attributed to corrosion by non-condensed brine as already discussed.

The comparison of the results from in-situ corrosion experiments with those from laboratory-scale studies [3] shows:

- The corrosion rates of the iron base alloys investigated in-situ have been much lower than those obtained in laboratory-scale experiments with brine in excess. The reason is the presence of limited amounts of brine in the in-situ experiments.
- For Ti 99.8-Pd and Hastelloy C4 only negligible differences have been found between laboratory and in-situ results of corrosion rates.
- The very pronounced local corrosion attacks on nodular cast iron, Ni-Resist D4, Si-cast iron and Hastelloy C4 (only at 200°C and under irradiation at 1000 Gy/h), respectively, observed in the laboratory-scale experiments have not occurred under the in-situ conditions due to the limited amounts of brine.

3.3 Testing of welded tubes in rock salt/brine at HLW design temperature

On the basis of the corrosion results and considering mechanical aspects a thick-walled steel container without or with corrosion protection made of Ti 99.8-Pd and Hastelloy C4, respectively, was selected for packaging of HLW. In accordance with these concepts two types of tube with simulated characteristics of container manufacturing were tested. They were:

Type I: a tube made of cast steel (GS 16 Mn 5) with the container closing technique simulated by electron beam welding.

Type II: two tubes made of cast steel with a corrosion protection layer of Ti 99.8-Pd and Hastelloy C4, respectively, applied by explosion plating and electron beam welding.

The chemical compositions of the tube materials are given in Tab. 1. Figure 17 shows the layout of the tubes. The tubes (specimens) consisted of nine sections (50 mm length, 45 mm outside diameter, 20 mm inside diameter) and a bottom part which were joined by electron beam welding. This gave tubes of 500 mm total length. After welding the non-corrosion protected cast-steel tube was subjected to thermal treatment for two hours at 700°C in order to simulate the cooling conditions applicable to the seam of a thick-walled container. More detailed information on tube manufacture is given in [3].

3.3.1 Test conditions and experimental set-up

The corrosion behaviour of the three tubes was tested under the conditions of hypothetical inflow of larger amounts of NaCl brine into the HLW boreholes during the initial disposal phase, i.e., while the annular gap between the container and the borehole wall was still open. For this, the tubes (700 cm² surface each) were placed into heated vertical boreholes of 2 m depth at the 775 m level of the Asse mine (see Fig. 18), and the 1 mm wide annular gap between the tubes and the borehole wall was filled with 100 ml saturated NaCl brine (26.9 wt.% NaCl, 73.1 wt.% H₂O). This gave a ratio of specimen surface to brine volume (S/V) of 7 cm⁻¹ which is greater by a factor of about 700 than that in the experiments of the Brine Migration Test. The maximum temperature of 200°C at the borehole wall (conforming to the German disposal concept) was set with a heater.

Figure 19 shows the radial temperature distribution between two boreholes in the center of the heated zone. The vertical temperature profile developing during the experiment at the contact surface between the tubes and the borehole wall is shown in Fig. 20. The maximum temperature of 200°C occurred in the center of the heated zone, and the minimum temperature of 90°C occurred in the upper tube zone. The temperatures were measured with NiCr-Ni thermocouples. In order to avoid invalidation of the corrosion measurements due to corrosion induced by contact between the thermocouples and the tube surface, the measurements were performed in reference boreholes of identical experimental set-up. The pressure in the annular gap of the real test boreholes were measured continuously with a manometer which was introduced into the brine inlet tube. The

maximum pressure measured was 0.28 MPa which corresponds to a boiling point of the salt brine of 140°C. This means that the water contained in the brine evaporated at points of elevated temperature and recondensed at the upper cooler end of the tubes (90°C).

The tensions prevailing on the tube surfaces were measured, like the temperature, in reference boreholes using strain gauges. The measurements have shown that the first contact of the borehole wall with the tubes due to rock pressure occurred after about six months. On the basis of results obtained in an identical preliminary test [3] complete closure of the 1 mm wide annular gap should have taken place after approximately twelve months.

3.3.2 Post-test investigation of the tubes

After a testing period of 18 months the tubes were retrieved by overcoring. The obtained drilling cores (1 m length, 120 mm outside diameter) had been cut into two half-shells (Figs. 21 and 22) and a visual inspection was made of the tubes and the drilling cores. No corrosion products were visible on the tubes protected by Ti 99.8-Pd and Hastelloy C4, respectively. Loosely attached corrosion products were found on the non-corrosion protected cast-steel tube. These were removed mechanically from each tube section and the tube bottom and examined by X-ray diffraction analysis. Then the tubes were pickled in suitable solutions and cleaned with alcohol in order to remove the salts and corrosion products left. After cleaning the tubes were subjected to post-test examinations for corrosion attacks by surface profilometry and metallography.

3.3.3 Results and discussion

Visual inspection of the drilling cores cut into two parts showed that the 1 mm annular gap between the tubes and the borehole wall which existed at the beginning of the tests had completely closed. Damp and shining zones of the cutting faces of the drilling cores are proof that the NaCl brine added had not been completely consumed by corrosion. Below the ceramic insulation in the cooler upper part of the tubes ($T = 90^{\circ}\text{C}$) dissolved salt was clearly visible which is attributed to condensation of water vapour. Furthermore, black and rust-brown corrosion products were uniformly distributed on the non-corrosion protected cast-steel tube and the borehole wall which indicates that iron oxides had been formed.

X-ray diffraction analysis has shown that the corrosion products loosely attached to the cast-steel tube consisted of a mixture of iron oxides and NaCl incorporated in the corrosion layer. The identified oxides were: Fe_3O_4 , Fe_2O_3 , $\alpha\text{-FeO(OH)}$ and $\gamma\text{-FeO(OH)}$. The ferric oxides and hydroxides present in addition to Fe_3O_4 found by Westerman et al. [8] are attributed to the presence of some oxygen in the in-situ experiment. No relationship has been found to exist between the composition of the corrosion products and the temperature of the specimens.

The surface profiles (Fig. 23) and the metallographic sections (Fig. 24) of specimens taken from three characteristic temperature zones (90°C, 140°C, 200°C) of the non-corrosion protected cast-steel tube have shown that corrosion attack was partly non-uniform and different in extent. Besides specimen areas where uniform corrosion had taken place, there were those which had suffered from deeper corrosion attacks. The corrosion attack was greatest for the specimens from the cooler upper part of the tube ($T = 90^\circ\text{C}$) where the evaporated water of the salt brine condensed. In that case, the maximum rate of penetration of corrosion was 120 $\mu\text{m/a}$. For the specimens taken from the zones at 140°C and 200°C in the vapour space the penetration rates were much lower, namely 20 $\mu\text{m/a}$, and differed slightly from each other. Pitting and crevice corrosion in the sense of an active-passive corrosion element or stress-corrosion cracking have not occurred at any point of the cast-steel tube. Electron beam welding did not noticeably influence the corrosion of steel.

The examination of the cast-steel tubes provided with a corrosion protection of Ti 99.8-Pd and Hastelloy C4, respectively, with the stereo-microscope and surface profilometry have not shown any changes on the surface of the plating materials by corrosion attacks. Neither on the mechanically finished surface nor on the hot-rolled and electron beam welded sheet metal surface (Fig. 25) were any signs of local corrosion observed. Also a crack produced by a steel needle in order to simulate severe conditions due to handling of the containers did not stimulate a corrosion attack. Figure 26 shows surface profiles of Ti 99.8-Pd and Hastelloy C4 before and after storage.

3.4 Testing at elevated temperature and in an elevated gamma radiation field

The conditions of HLW test disposal in 15 m deep cased boreholes in the Asse salt mine [10] at $T = 200^\circ\text{C}$ - 250°C and a maximum gamma dose-rate of 5×10^3 Gy/h on

the surface of the casing allow packaging materials to be examined at elevated temperatures and in an elevated gamma-radiation field. Both the temperature of 250°C and the dose rate of 5×10^3 Gy/h should be considered as overtest conditions for the thick-walled HLW packaging discussed (200°C, about 1-10 Gy/h). Moreover, it will be possible to perform in the planned dummy canisters experiments at low temperatures and at different gamma dose-rates. Also, the Ti 99.8-Pd liner used upon recommendation of KfK as a corrosion protection of the steel casing will offer a unique opportunity to study on a technical scale a simulated HLW overpack.

For these reasons detailed corrosion studies had been planned by KfK as early as in the test definition phase. The following investigations will be performed in the course of HLW test disposal which will start in 1990 and last 5 years:

- Investigation of metal sheets of selected packaging materials at $T_{\max} = 200^\circ\text{C}$ - 250°C without irradiation and at 5×10^3 Gy/h gamma dose-rate. For this purpose, specimens have been provided on the external wall of the borehole casing. Due to the thermally induced borehole convergence to be expected (rock pressure about 40-45 MPa) a contact of the specimens with the borehole wall can be anticipated to occur within a short period. Besides the promising HLW packaging materials fine-grained steel, Ti-99.8-Pd and Hastelloy C4, tantalum and Cr-Ni-steel 1.4833 will be investigated. This steel grade will be used in the reprocessing plants of La Hague (COGEMA) and Sellafield (BNFL) as material for HLW canisters.
- Investigation of the materials above in loose rock salt with different H₂O contents (< 0.1 wt.% to 1 wt.%) at $T = 90^\circ\text{C}$ - 150°C and gamma dose-rates between 10^3 Gy/h and 10^5 Gy/h. For this, the specimens and corrosion medium are placed into glass ampoules and positioned at different levels in the dummy canisters.
- Investigation of the corrosion protection material (Ti 99.8-Pd) of the casing with a view to the influence exerted on corrosion by the conditions of manufacture applying to a simulated HLW overpack. The characteristic details of manufacture of borehole casing have been entered in Fig. 27.

Figure 28 shows a longitudinal section of a cased borehole used for disposal as well as the positioning of the material specimens to be investigated. The speci-

mens on the external wall of the casing were fixed in ceramic insulated pockets provided in the coupling sleeves of the casing (Fig. 29).

After completion of the 5 years testing period the material specimens and the liner material of the casing, Ti 99.8-Pd, will be examined for corrosion attacks by means of gravimetry, surface profilometry and metallography. The characterisation of rock salt in terms of chemistry and mineralogy prior to the beginning of the test, which is required in order to allow the corrosion results to be interpreted at a later date, has already been performed. Detailed information about that characterisation can be taken from [14].

4. Conclusions

The unalloyed steels (fine-grained steel, low-carbon and cast-steel) investigated exhibited non-uniform general corrosion in the two-phase corrosion media rock salt /rock-salt brine and rock salt/Q-brine at 90°C and 170°C without irradiation. Pitting or crevice corrosion in the sense of an active-passive corrosion element which would put in doubt the use of the steels as HLW container materials have not been observed.

Little differences have been found between the corrosion rates of the steels in the above-mentioned media at both temperatures, except for the corrosion rate of cast steel in rock salt/Q-brine at 170°C. In this case, it was about twice that of the two hot-rolled steels. By increase in temperature from 90°C to 170°C, the corrosion rates of the steels in both media rose by about a factor of 2, whereas the values in rock salt/Q-brine were about twice those in rock salt/rock salt brine. The maximum corrosion rates obtained for the reference fine-grained steel in the most aggressive medium, rock salt/Q-brine, at 90°C and 170°C imply corrosion allowances on the order of 25 mm to 50 mm for the containers discussed here with 300 years service life.

Gamma-dose rates of 1 Gy/h-100 Gy/h did not influence noticeably the corrosion behaviour of the steels in all test media (rock salt/brines, Q-brine) at 90°C. No increase in corrosion rates over those in the experiments without irradiation and no pitting and crevice corrosion or stress-corrosion cracking were observed. Furthermore, the maximum corrosion rates of the steels (50 $\mu\text{m/a}$ -60 $\mu\text{m/a}$) were inter-comparable and did not differ significantly in either of the test media. Also welding (TIG, EB) or H₂S concentrations of 25 mg/l-200 mg/l in Q-brine did not enhance

noticeably the corrosion rates of the steels at 90°C-170°C. In case of Hastelloy C4 pitting and crevice corrosion occurred in Q-brine at gamma dose-rates higher than 1 Gy/h and H₂S concentrations of 25 mg/l, respectively. These results are in agreement with previous electrochemical studies [15].

In the in-situ experiments performed in rock salt and in rock salt/limited amounts of NaCl brine (Brine Migration Test) no noticeable corrosion of the materials investigated (Fe-base materials, Ti 99.8-Pd, Hastelloy C4) was observed. This is true above all for Ti 99.8-Pd and Hastelloy C4 undergoing passive corrosion and in which local corrosion could be caused already by minor amounts of brine. Furthermore, a gamma dose-rate of 3x10² Gy/h or TIG welding did not influence the corrosion behaviour of the materials. Nevertheless, the materials Ni-Resists D2 and D4, cast iron and Si-cast iron must be excluded as HLW container materials because in laboratory studies [3] performed with MgCl₂-rich brine (Q-brine) in excess they proved to be susceptible to pitting and intergranular corrosion.

.In the in-situ testing of cast-steel tubes without and with corrosion protection made of Ti 99.8-Pd and Hastelloy C4, respectively, in rock salt/larger amounts of NaCl brine, no influence of container manufacturing characteristics (EB welding, explosion plating, etc.) on corrosion was observed. Examinations of the tubes did not show any detectable corrosion attacks of the plating materials. Cast steel corroded non-uniformly at a maximum corrosion rate of 120 μm/a which implies acceptable corrosion allowances for the thick-walled containers discussed here. Furthermore, no pitting and crevice corrosion or stress-corrosion cracking occurred on the cast-steel tube.

In general, it can be stated that the laboratory and in-situ corrosion results are in good agreement and that they confirm the promising nature of unalloyed steels and Ti 99.8-Pd as materials for long-term resistant HLW packagings. Further corrosion studies on these materials are in progress. They focus on the clarification of the role which high temperature ($\leq 200^{\circ}\text{C}$) plays during corrosion under gamma irradiation and on the performance of statistical in-situ experiments. In these in-situ experiments areas with variations in the composition of salt minerals will be selected in order to extend the statistical basis of the corrosion data.

4. Literatur

- [1] E. Smailos, "Korrosionsuntersuchungen an ausgewählten metallischen Werkstoffen als Behältermaterialien für die Endlagerung von hochradioaktiven Abfallprodukten in Steinsalzformationen ", KfK-Report 3953 (1985).
- [2] G.P. Marsh, G. Pinard-Legry, E. Smailos et al., "HLW container Corrosion and Design", Proc. of the 2nd European Community Conference on Radioactive Waste Management and Disposal, Luxembourg, April 22-26, 1985, p. 314. Cambridge University Press (1985).
- [3] E. Smailos, W. Schwarzkopf, R. Köster, "Corrosion Behaviour of Container Materials for the Disposal of High-Level Wastes in Rock Salt Formations", Nuclear Science and Technology, CEC-Report, EUR 10400 (1986).
- [4] G.H. Jenks, "Radiolysis and Hydrolysis in Salt-Mine Brines", ORNL/TM-3717, Oak Ridge National Laboratory (1972).
- [5] E. Smailos, R. Köster, "Materials Reliability in the Back End of the Nuclear Fuel Cycle", Proc. of a Technical Committee Meeting of IAEA, Vienna, Austria, September 2-5, 1986, IAEA-TECDOC-421, p. 7 (1987).
- [6] R. Köster, "Ausgewählte Aspekte der Endlagerung radioaktiver Abfälle in Steinsalzformationen", Schriftenreihe der Universität Regensburg, Band 13, p. 71 (1986).
- [7] W. Hauser, Kernforschungszentrum Karlsruhe, unpublished results.
- [8] R.E. Westerman, J.H. Haberman et. al., "Corrosion and Environmental-Mechanical Characterisation of Iron-Base Nuclear Waste Package Structural Barrier Materials", PNL-5426 (1986).
- [9] T. Rothfuchs, "In-Situ Investigations on the Impact of Heat Production and Gamma Radiation with Regard to High-Level Radioactive Waste Disposal in Rock-Salt Formations", Nuclear Technology, 74, p. 209 (1986).

- [10] K. Kühn, T. Rothfuchs, "In-Situ Experiments on the Disposal of High-Level Radioactive Wastes at the Asse Salt Mine, Federal Republic of Germany", Proc. of Waste Management'89, Tucson, Arizona, February 26-March 2, 1989, Vol. 1, p. 567 (1989).
- [11] E. Smailos, R. Köster, W. Schwarzkopf, "Korrosionsuntersuchungen an Verpackungsmaterialien für hochaktive Abfälle", European App. Res. Rept. - Nuclear Science Technology, Vol. 5, No. 2, p. 175 (1983).
- [12] A. Pudewills, E. Korthaus, R. Köster, "Model Calculations of the Thermo-mechanical Effects in the Near Field of a High-Level Radioactive Waste Repository", Nuclear Technology, No. 82, p. 71 (1988).
- [13] T. Rothfuchs et al., "Nuclear Waste Repository Simulation Experiments", GSF-Report T-260 (1986).
- [14] H. Gies, N. Jockwer, J. Monig, "Geochemistry of the HAW Test Field and Occurrence of Primary and Secondary Gases", Proc. of Waste Management '89, Tucson, Arizona, February 26-March 2, 1989, Vol. 1, p. 615 (1989).
- [15] R.E. Schmitt, R. Köster, "Elektrochemische Korrosionsuntersuchungen an metallischen Verpackungsmaterialien für hochaktive Abfälle", KfK-Report 4039 (1986).

Table 1 Chemical compositions of the materials tested on the laboratory-scale and in-situ corrosion experiments

Material	Composition (wt.%)										
	Cr	Ni	Mo	Ti	Pd	C	Si	Mn	O ₂	H ₂	Fe
Ti 99.8-Pd Material No. 3.7025.10	-	-	-	Bal.	0.18	0.01	-	-	0.04	0.001	0.05
Hastelloy C4 Material No. 2.4610	15.4- 16.8	Bal.	15.2- 15.9	0.33	-	0.006	0.05	0.09	-	-	0.05
Fine-grained steel Material No. 1.0566	-	-	-	-	-	0.17	0.44	1.49	-	-	Bal.
Low-carbon steel	-	-	-	-	-	0.1	0.27	0.66	-	-	Bal.
Cast steel Material No. 1.1131	-	-	-	-	-	0.16	0.61	1.51	-	-	Bal.
Nodular cast iron Material No. 0.7043	-	-	-	-	-	3.7	1.83	0.21	-	-	Bal.
Ni-Resist D2 Material No. 0.7660	2.39	22	-	-	-	2.65	2.4	1.14	-	-	Bal.
Ni-Resist D4 Material No. 0.7680	5.5	30.9	-	-	-	2.6	4.25	0.5	-	-	Bal.
Si-cast iron	-	-	-	-	-	0.72	15.0	0.62	-	-	Bal.

- = not existing or negligible

Table 2 Chemical compositions of salt brines used in the laboratory-scale corrosion experiments

Ions/elements	Asse rock-salt-brine ¹⁾ (g/l at 25°C)	Q-Brine ²⁾ (g/l at 55°C)
Na ⁺	136.75	7.1
K ⁺	1.48	31.8
Mg ²⁺	0.34	91.9
Ca ²⁺	1.40	-
Sr ²⁺	0.01	-
B	0.007	-
Al	0.003	-
Zn + Fe + Li ⁺	<0.001	-
Cl ⁻	201.9	297.3
SO ₄ ²⁻	5.19	14.4

- 1) pH (25°C) = 6.1 ± 0.2; saturated O₂-concentration (25°C) = 5.8 mg/l.
- 2) pH (25°C) = 4.9 ± 0.2; saturated O₂-concentration (25°C) = 3.7 mg/l.

Table 3 Test conditions for unalloyed steels and Hastelloy C4 in the laboratory-scale corrosion experiments (maximum test duration: 1 year)

Comparative studies on fine-grained steel, low-carbon steel and cast steel		
Corrosion medium	Temperature (°C)	Gamma dose-rate (Gy/h)
Asse rock-salt plus Asse rock-salt brine	90, 170	-
Asse rock-salt plus Q-brine	90, 170	-
Q-brine	90	1; 10
Additional studies on fine-grained reference steel		
Asse rock-salt plus Asse rock-salt brine	90	1; 10
Asse rock-salt plus Q-brine	90	1; 10
Q-brine	90	100
Q-brine and Q-brine plus H ₂ S (25, 100, 200 mg/l)	170	-
Studies on Hastelloy C4		
Q-brine	90	1; 10; 100
Q-brine and Q-brine plus 25 mg H ₂ S/l	150	-

Tab. 4 General corrosion rates and maximum pitting rates of Hastelloy C4 after 1 year immersion in Q-brine at 90°C with and without gamma irradiation

Dose rate (Gy/h)	Average general corrosion rate (µm/a)	Maximum pitting corrosion rate (µm/a)
0	0.1	-
1	0.05	-
10	0.4	20
100	0.4	20
1000	3.5	1000

- = uniform corrosion

Table 5 Corrosion results on Hastelloy C4 at 150°C in Q-brine with and without addition of H₂S

Corrosion medium	Testing time (months)	General corrosion rate (µm/a)	Maximum pitting corrosion rate (µm/a)	Maximum rate of crevice corrosion ¹⁾ (µm/a)
Q-brine	2	0.9 ± 0.1	-	-
	6	0.5 ± 0.05	-	-
	12	0.7 ± 0.3	-	150
Q-brine plus 25 mg H ₂ S/l	2	3 ± 0.4	--	-
	6	4.1 ± 1.1	40	1000
	12	3.9 ± 0.6	2300	2200

¹⁾ below specimens suspended with PTFE threads

Table 6 Weight losses and corrosion rates of the materials tested in-situ in Asse rock-salt at 32°C rock temperature (3 years reference experiment)

Material	Material condition	Dimension of specimens (mm)	Weight loss ¹⁾ (g/m ²)	General ¹⁾ corrosion rate (µm/a)
Ti 99.8-Pd	A	40x20x4	-	-
	W		-	-
Hastelloy C4	A	40x20x4	-	-
	W		-	-
Fine-grained steel	A	40x20x4	1.32	0.06
	W		25.20	1.06
Nodular cast iron	A	50x10x10	3.0	0.14
Ni-Resist D2	A	50x10x10	1.47	0.06
Ni-Resist D4	A	50x10x10	0.37	-
Si-cast iron	A	40x20x5	-	-

A = as-delivered; W = TIG welded

1) average value of 3 specimens

- = no measurable corrosion attack

Table 7 Weight losses and corrosion rates of the materials tested in-situ in Asse rock-salt/
limited amounts of brine (Brine Migration Test)

Material	Test temperature (°C)	Without gamma-irradiation (exposure time: 900 d)		With gamma-irradiation 3x10 ² Gy/h (exposure time: 700 d)	
		Weight loss (g/m ²)	Corrosion rate (µm/a)	Weight loss (g/m ²)	Corrosion rate (µm/a)
Ti 99.8-Pd	210	+	+	1.4	0.16
Hastelloy C4	210	+	+	19.19	1.18
Fine-grained steel	150	17.79	0.95	200.06	13.68
Cast steel	150	22.72	1.18	9.49	0.63
Ni-Resist D4	150	5.43	0.29	3.23	0.22
Nodular cast iron	120	+	+	13.26	1.01
Si-cast iron	120	29.31	1.72	+	+

+ = Specimens not retrievable or mechanically damaged

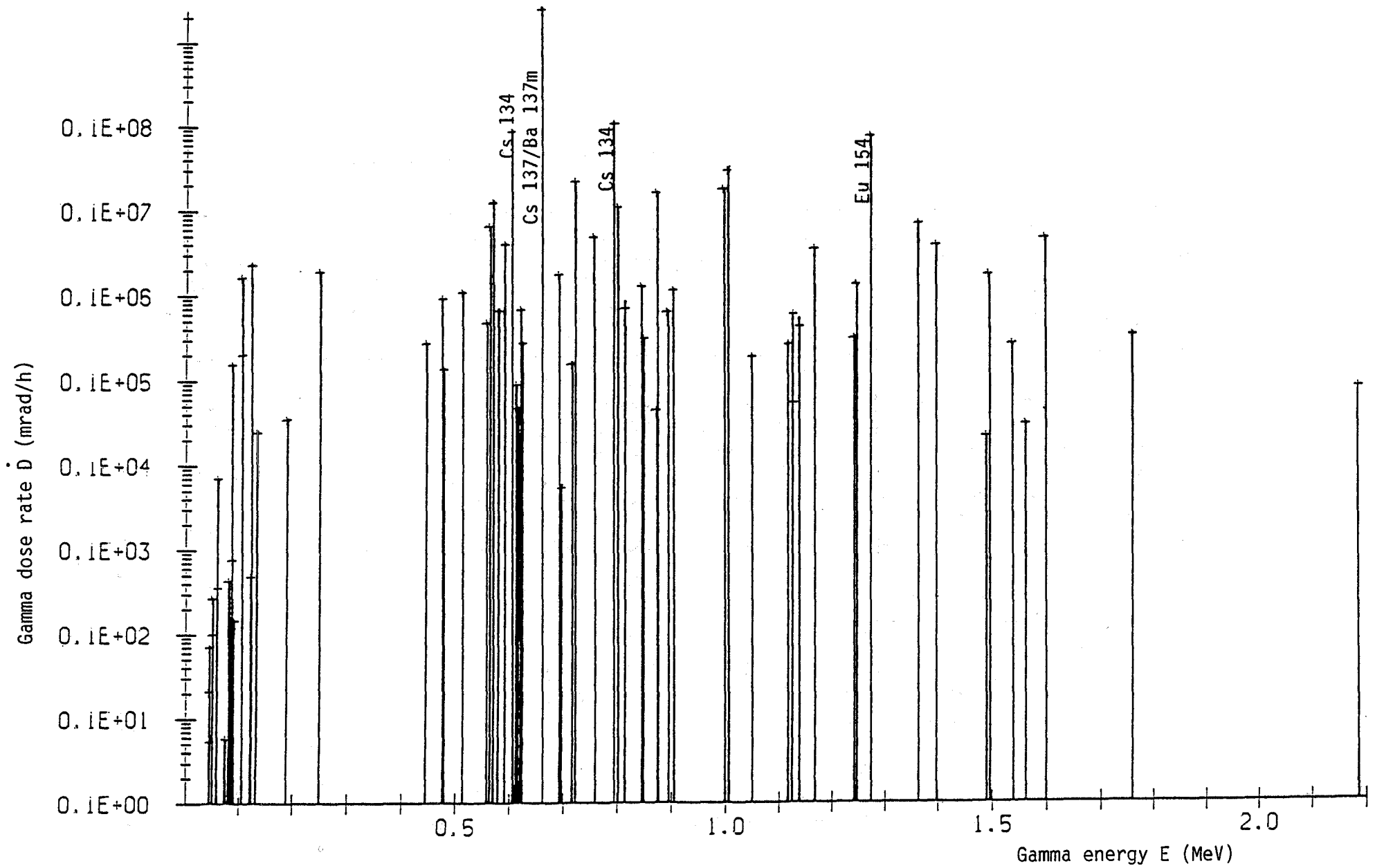


Fig. 1 Calculated gamma spectrum for 10 years old vitrified HLWC [7]

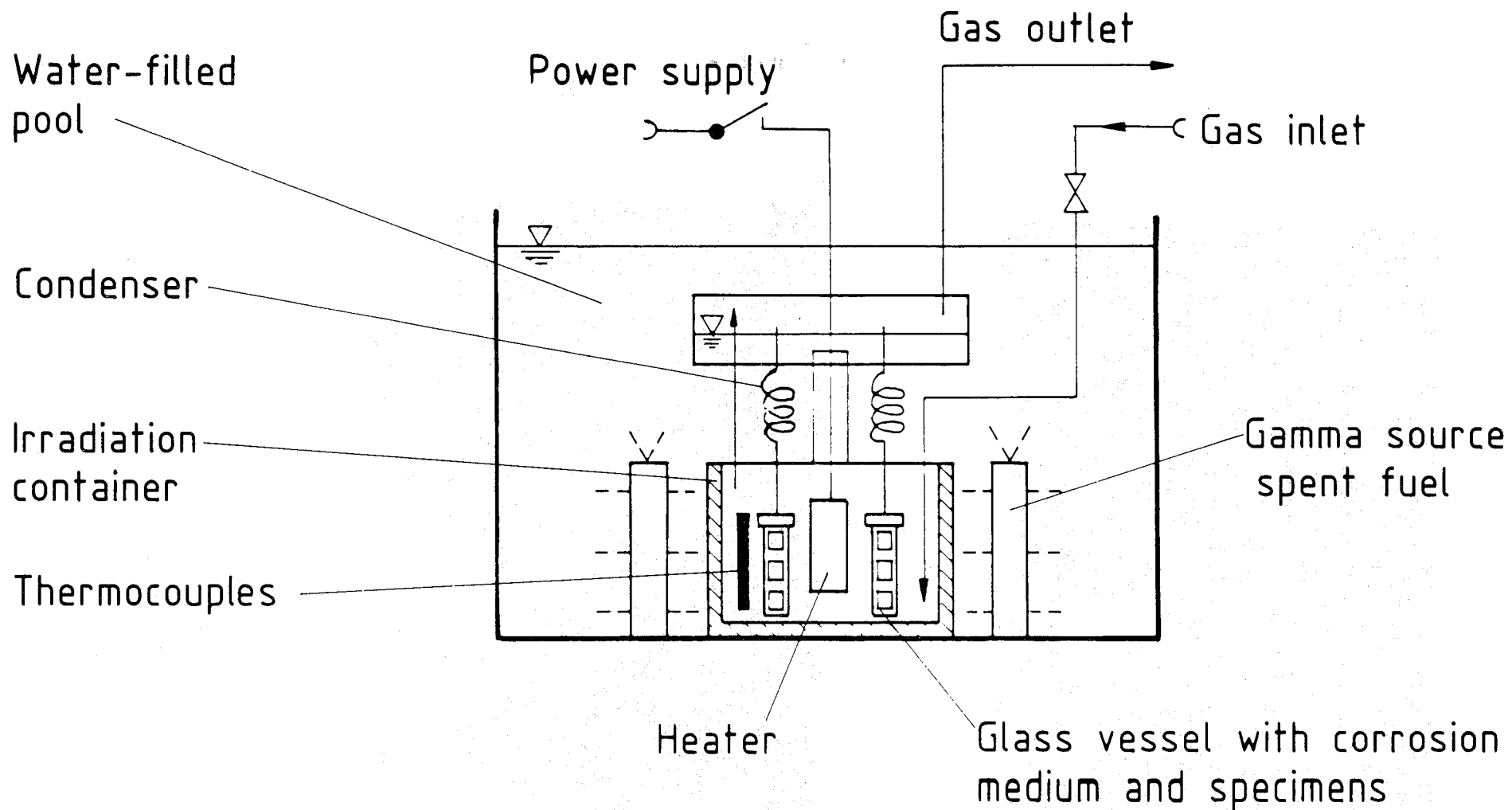
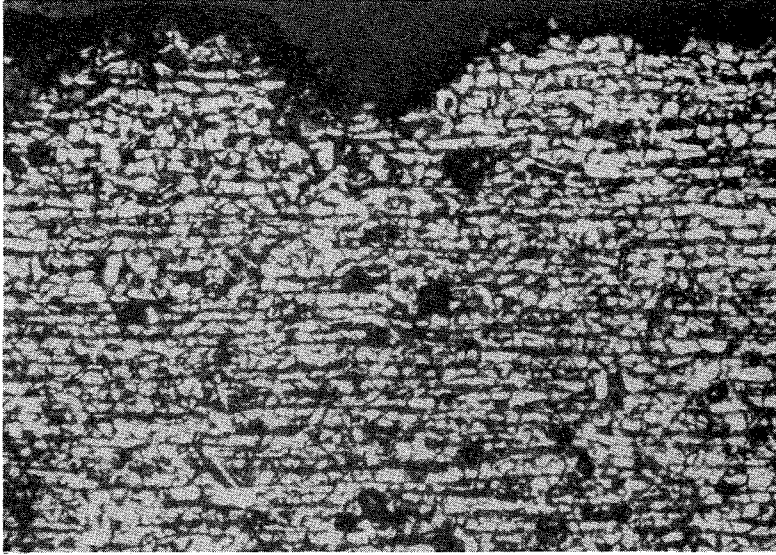
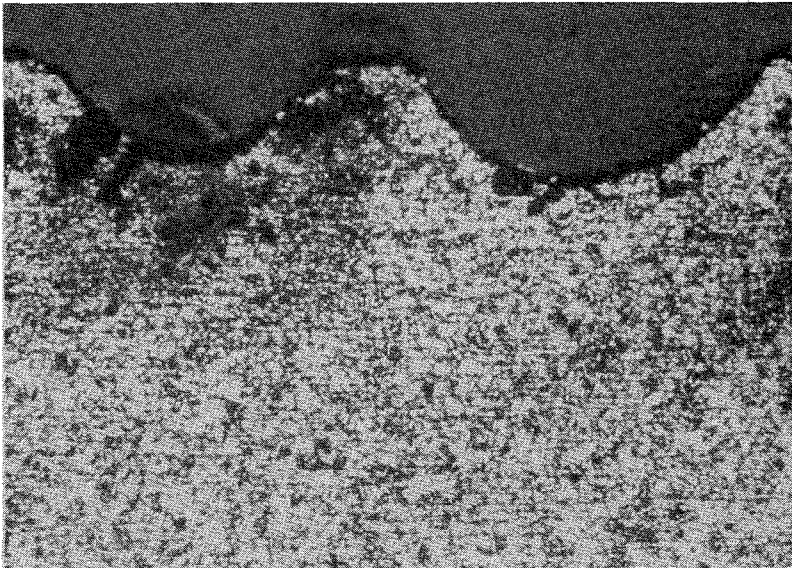


Fig. 2 Experimental set-up for corrosion studies under gamma irradiation at 90°C



x 200

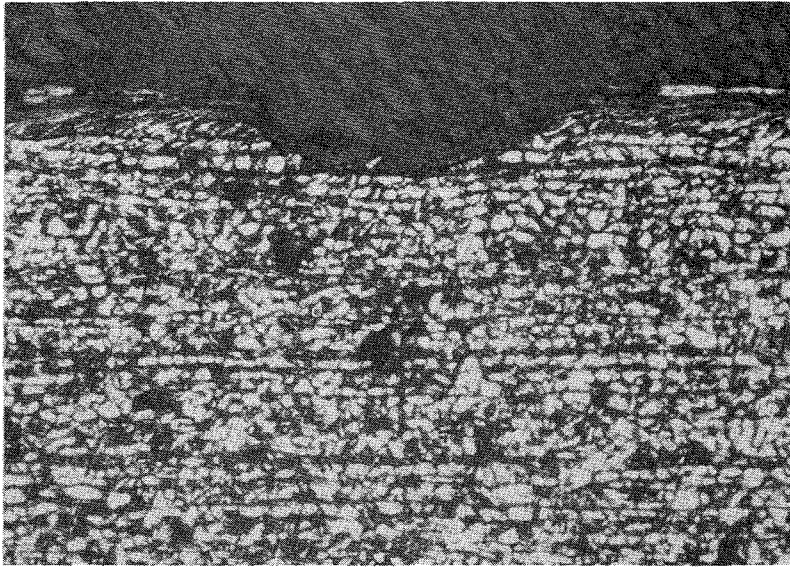
90°C



x 100

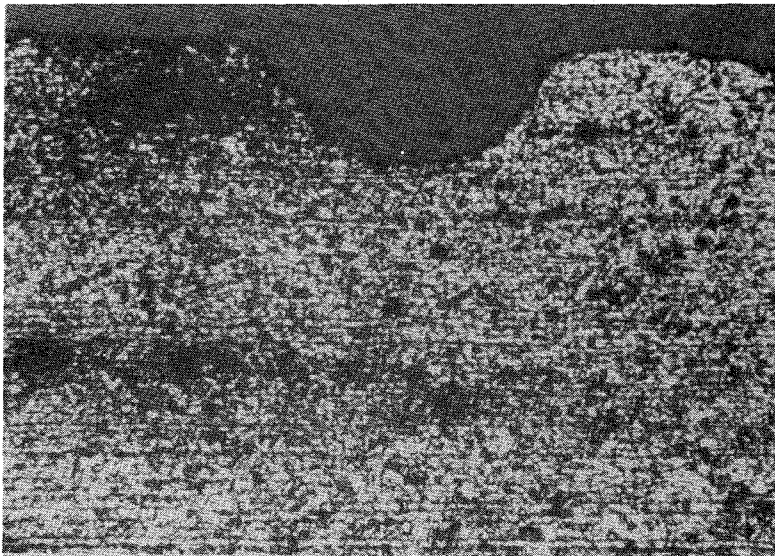
170°C

Fig. 3 Optical micrographs of fine-grained steel after 1 year in Asse rock-salt plus Asse rock-salt brine at 90°C and 170°C



x 200

90°C



x 100

170°C

Fig. 4 Optical micrographs of fine-grained steel after 1 year in Asse rock-salt plus Q-brine at 90°C and 170°C

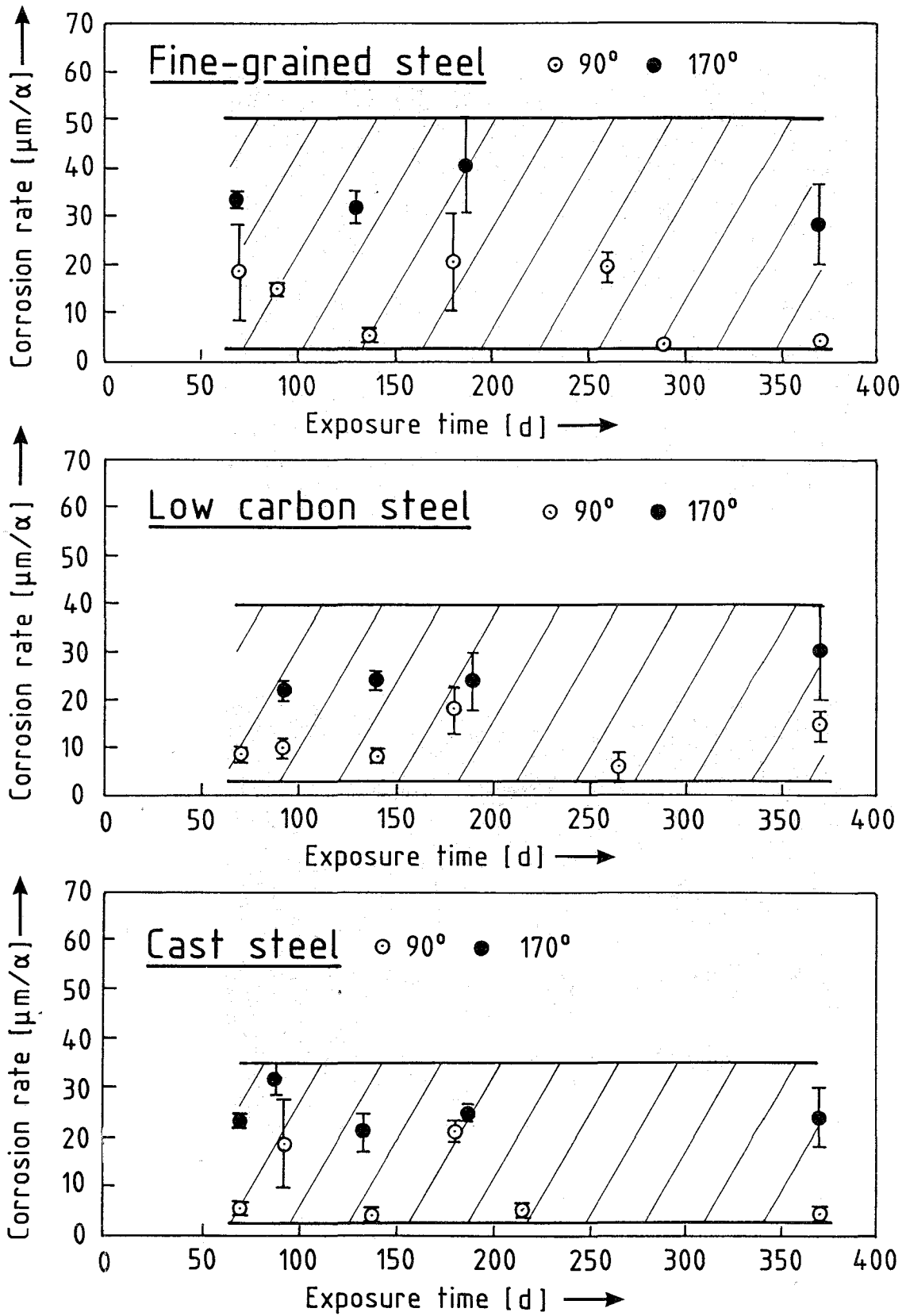


Fig. 5 General corrosion rates of unalloyed steels in Asse rock salt/Asse rock salt brine at 90°C and 170°C

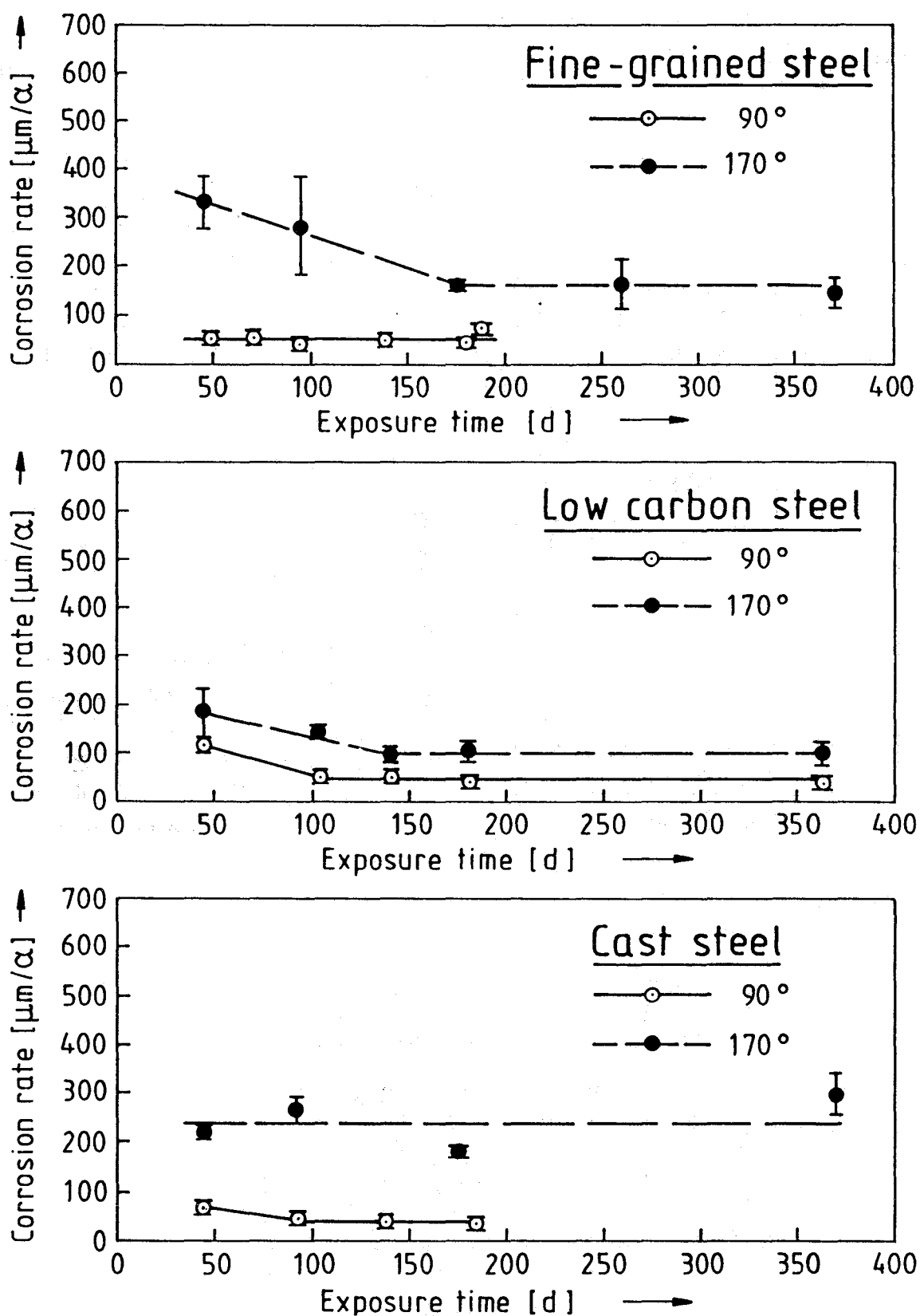


Fig. 6 General corrosion rates of unalloyed steels in Asse rock salt/Q-brine at 90°C and 170°C

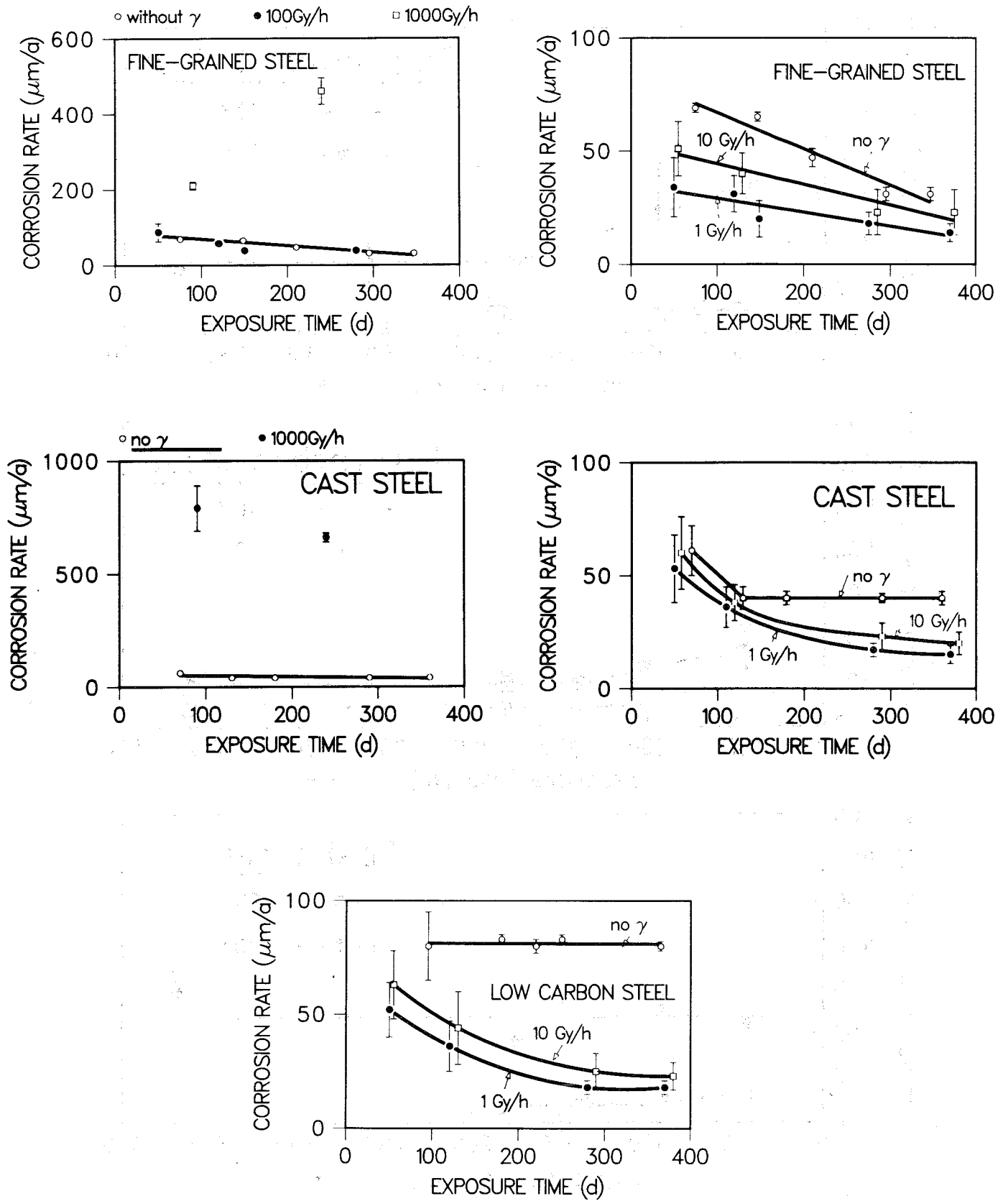


Fig. 7 Average general corrosion rates of unalloyed steels in Q-brine at 90°C with and without gamma irradiation

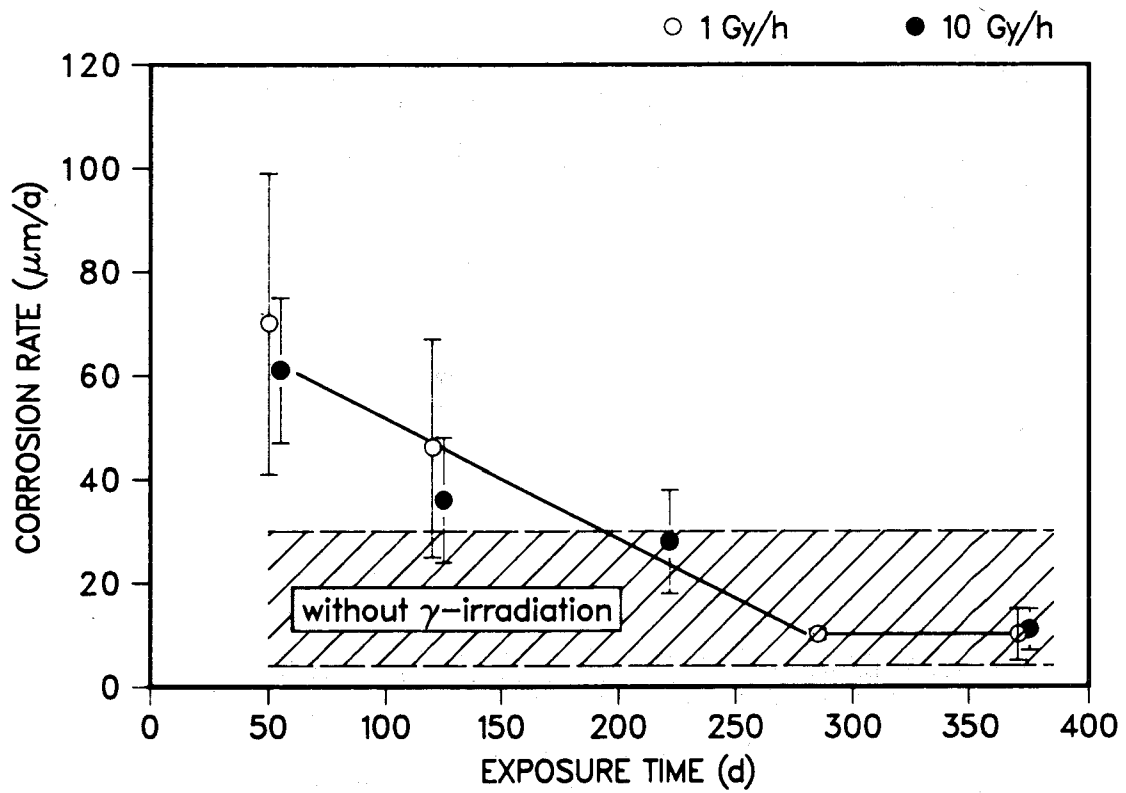


Fig. 8 General corrosion rates of fine-grained steel in Asse rock-salt/Asse rock-salt brine at 90°C with and without gamma irradiation

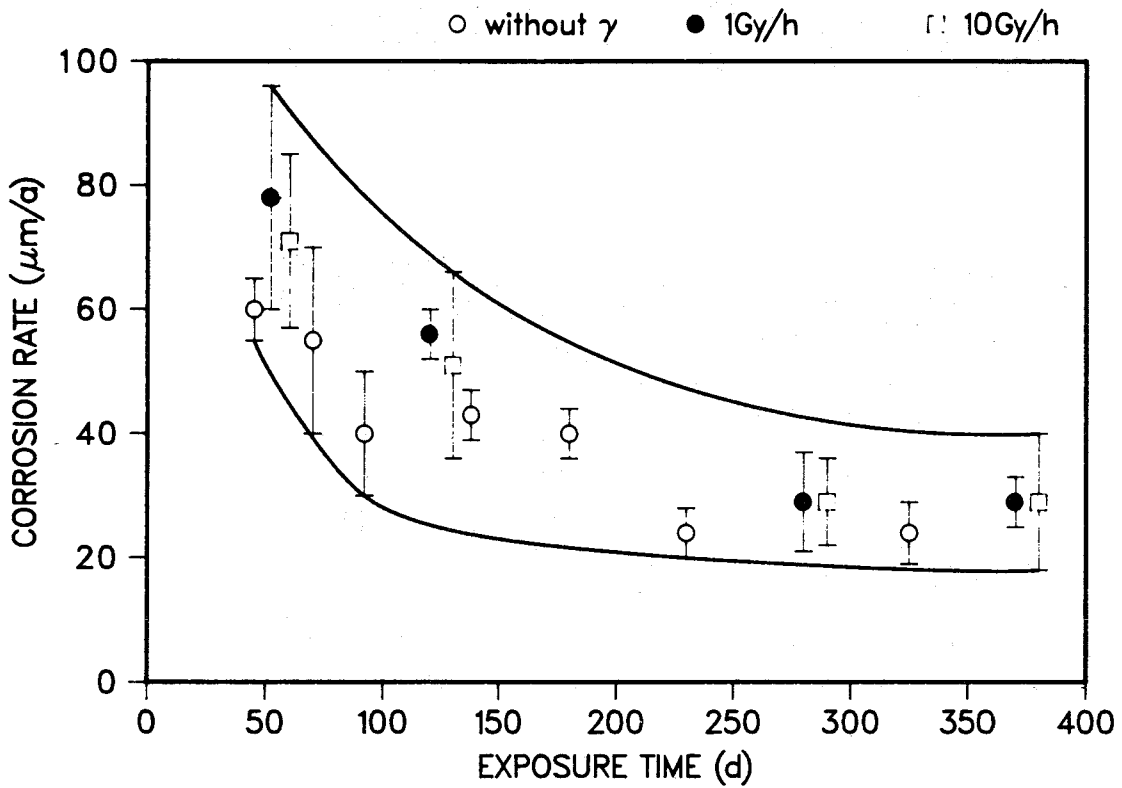
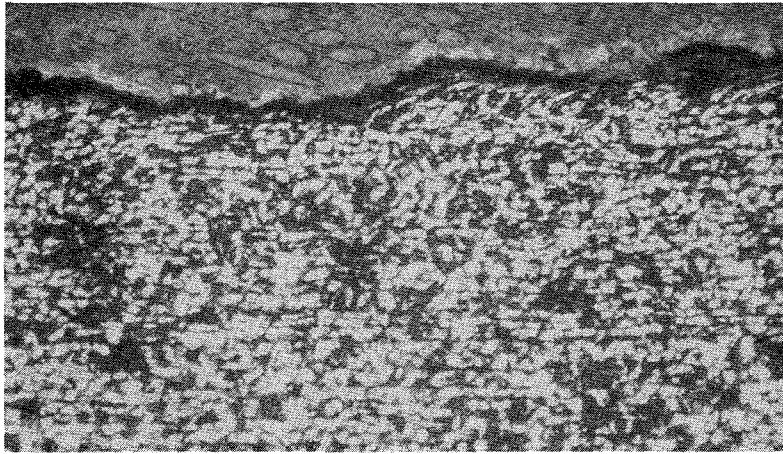
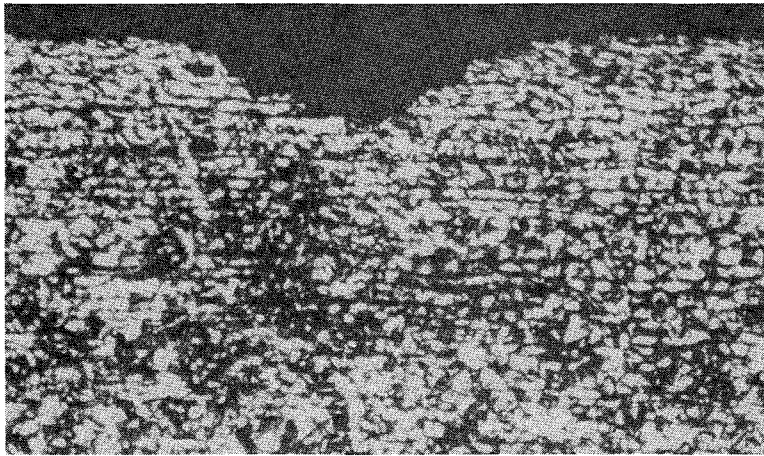


Fig. 9 General corrosion rates of fine-grained steel in Asse rock-salt/Q-brine at 90°C with and without gamma irradiation



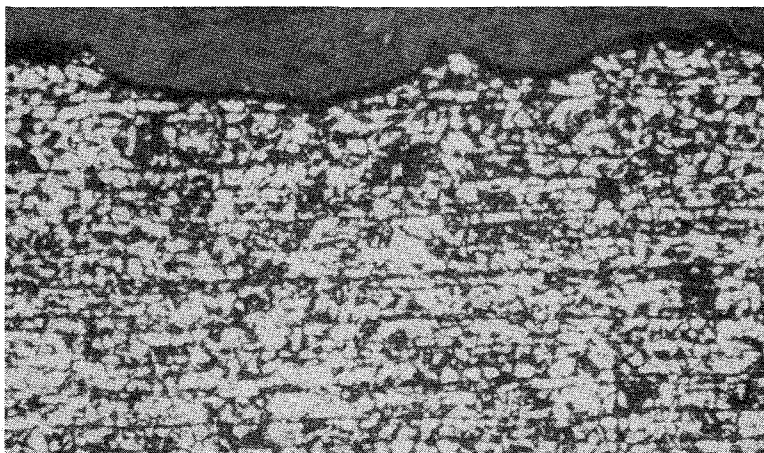
x 200

Q - brine



x 200

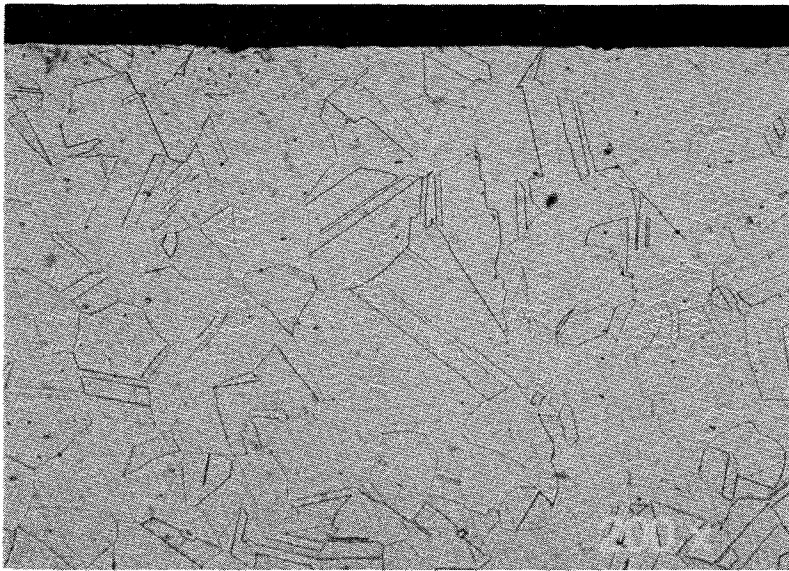
Asse rock-salt + Asse rock salt brine



x 200

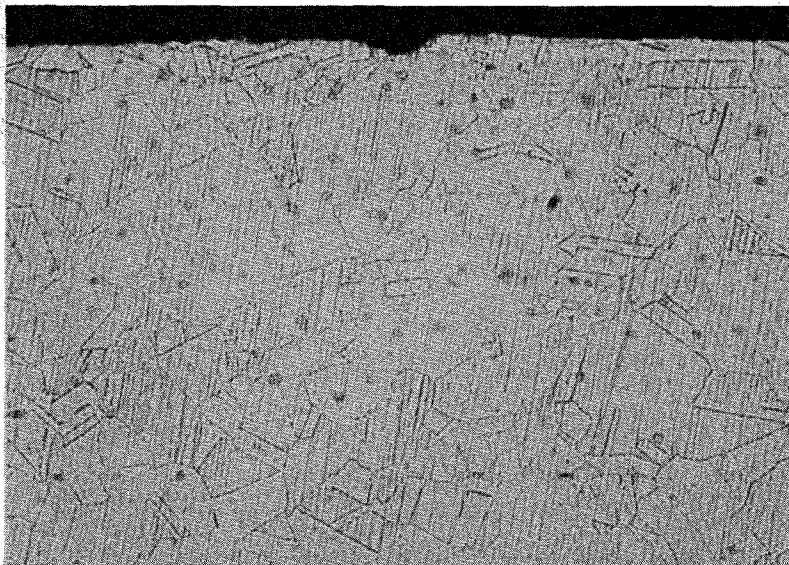
Asse rock-salt + Q-brine

Fig. 10 Optical micrographs of fine-grained steel after 1 year exposure in various corrosion media at 90°C and a gamma dose rate of 10 Gy/h



x 200

1 Gy/h



x 200

100 Gy/h

Fig. 11 Optical micrographs of Hastelloy C4 after 1 year immersion in Q-brine at 90°C and gamma dose rates of 1 Gy/h and 100 Gy/h

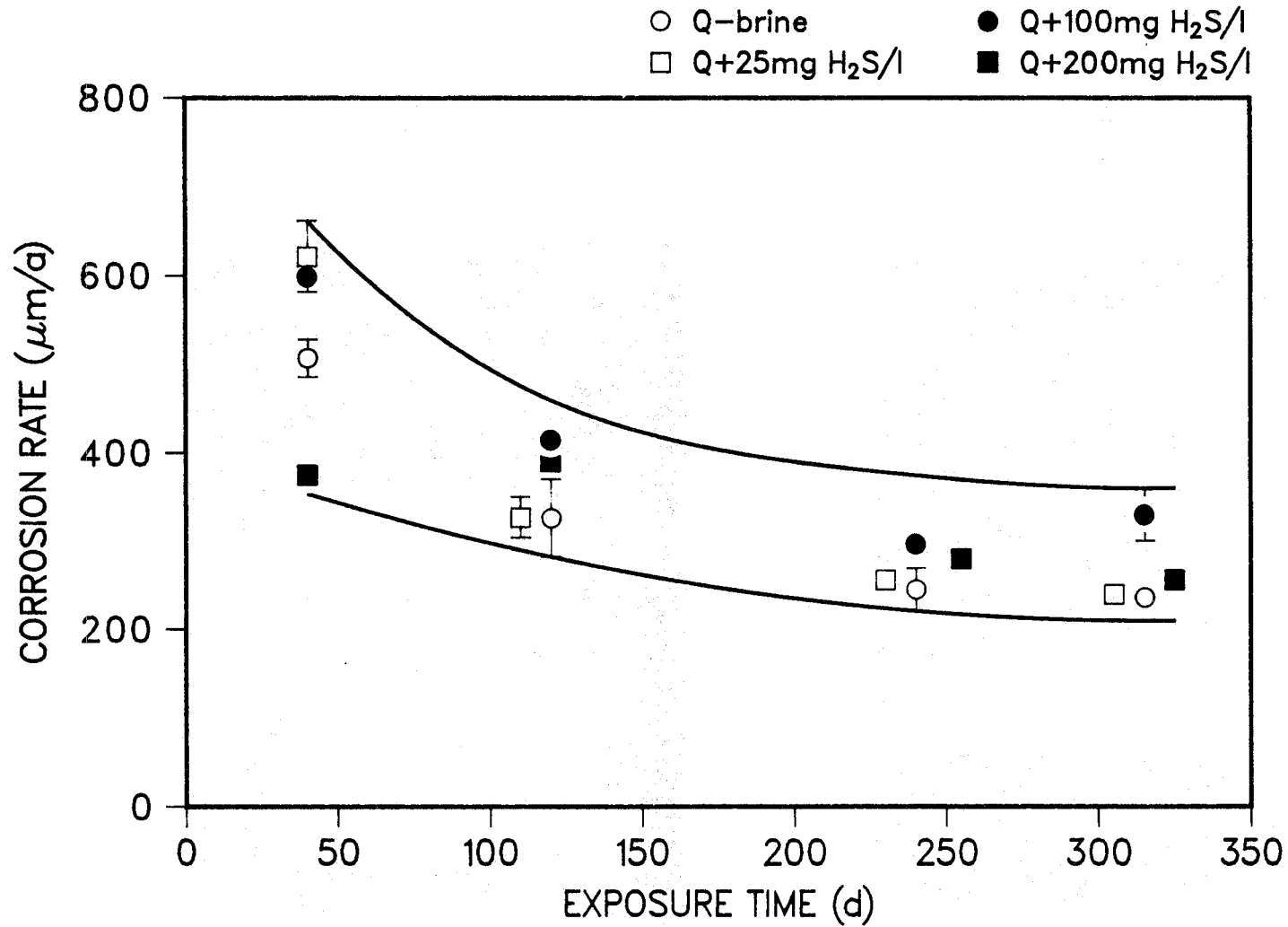
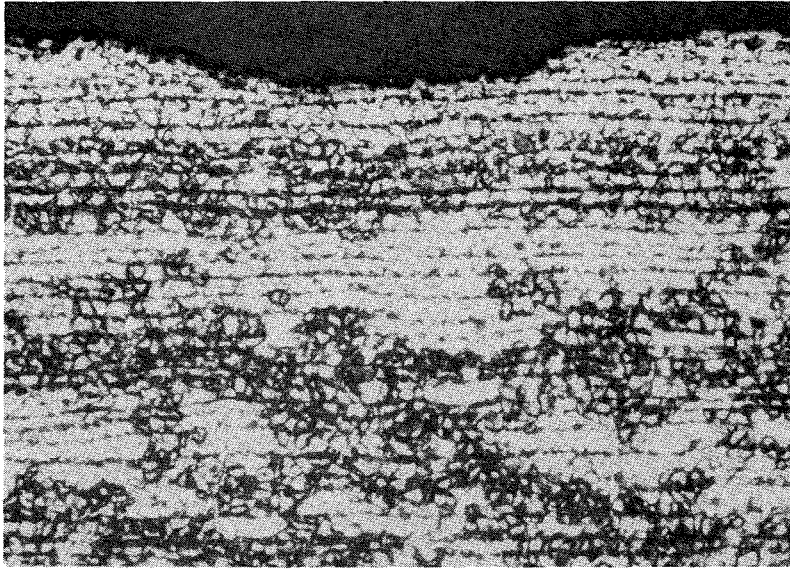
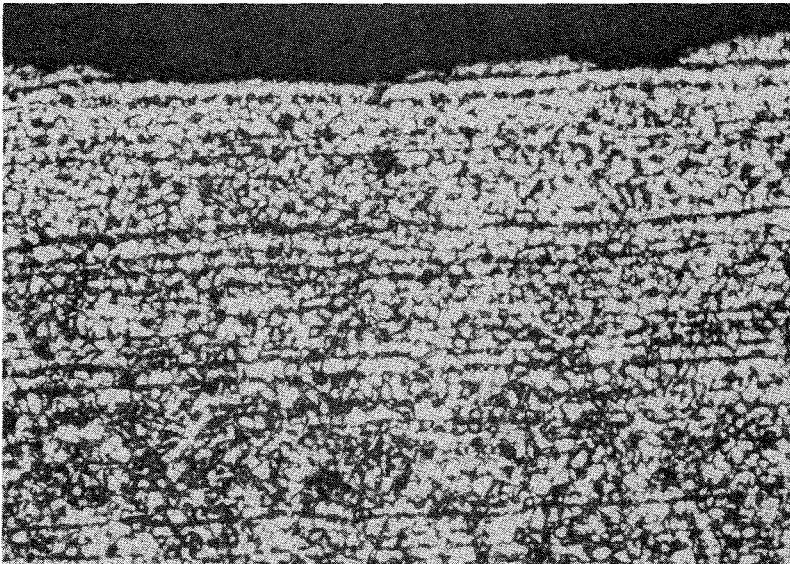


Fig. 12 Average corrosion rates of fine-grained steel in Q-brine with and without additions of H₂S at 170°C



x 200

Q-brine



x 200

Q-brine + 200 mg H₂S/l

Fig. 13 Optical micrographs of fine-grained steel after 325 days immersion in Q-brine and Q-brine + 200 mg H₂S/l at 170°C

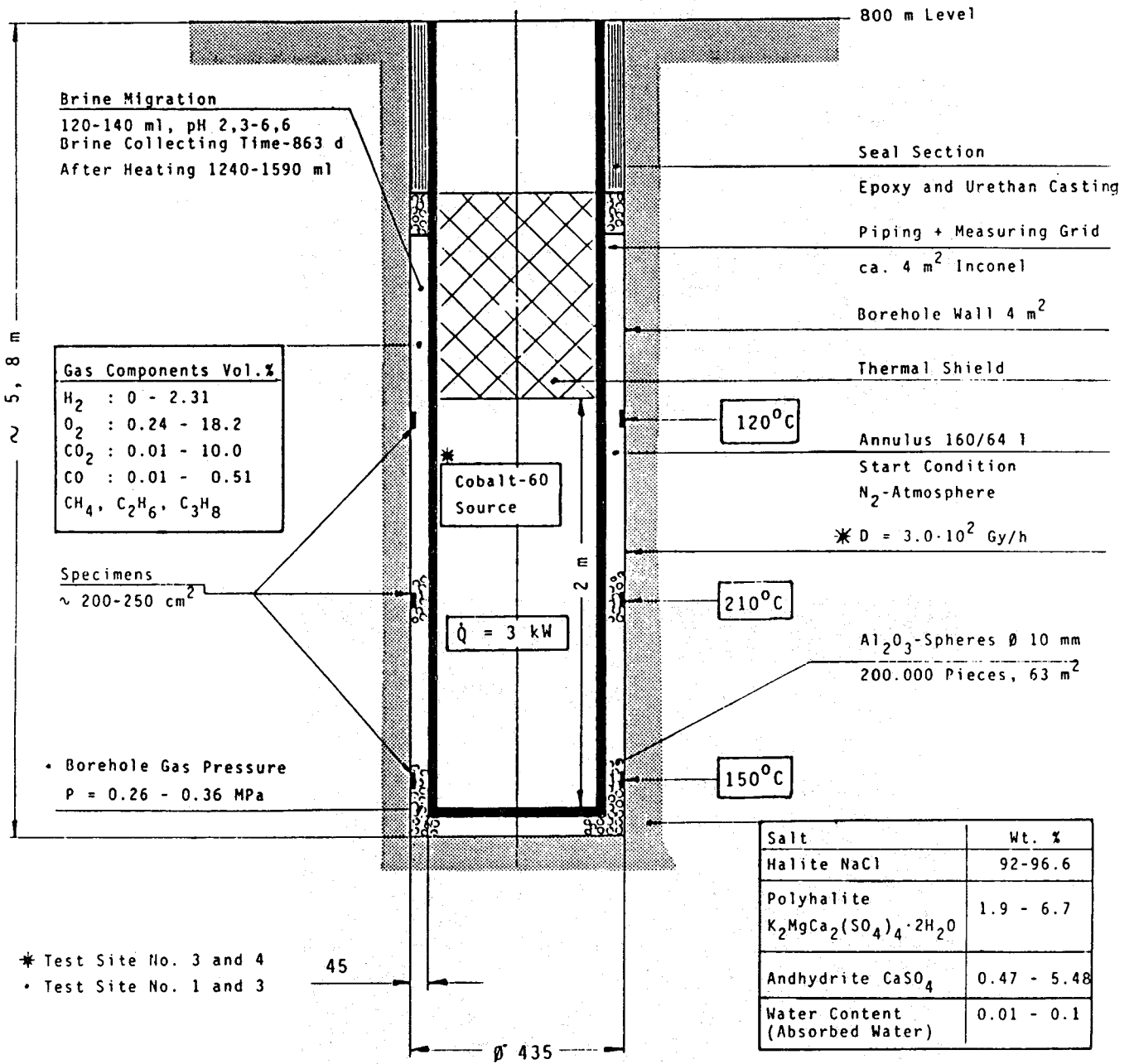
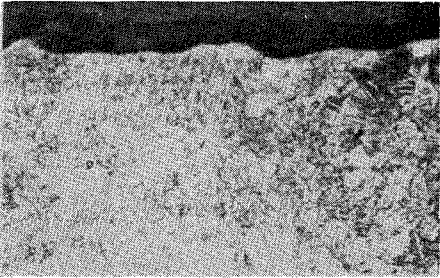
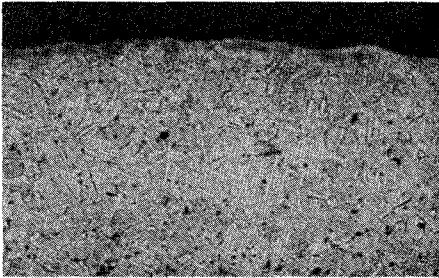
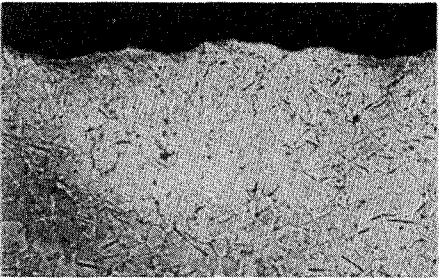
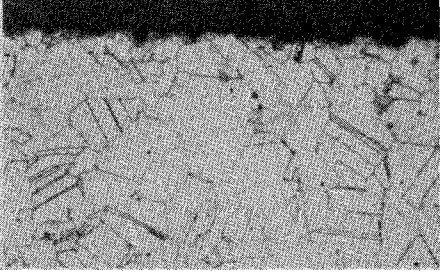
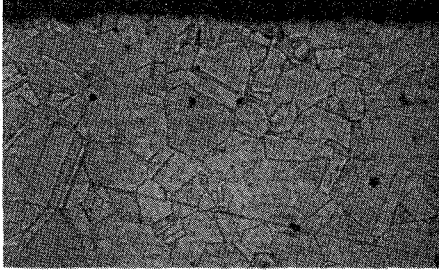
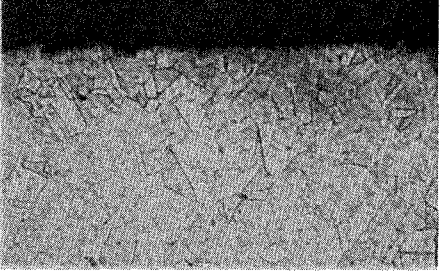
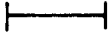



Fig. 14 Schematic vertical section of the test assembly with indication of the corrosion conditions (in-situ corrosion experiments carried out within the framework of the Brine Migration Test)

M A T E R I A L	Before Exposure	After Exposure without Gamma-Irradiation $T = 210^{\circ}\text{C}, \quad t = 900 \text{ d}$	After Exposure with Gamma-Irradiation $T=210^{\circ}\text{C}, t=700 \text{ d}, \dot{D} \text{ ca. } 3 \cdot 10^2 \text{ Gy/h}$
Ti 99.8-Pd			
Hastelloy C4			


0.1 mm


0.1 mm



0.1 mm

Fig. 15 Optical micrographs of Ti 99.8-Pd and Hastelloy C4 stored in the Brine Migration Test

MATERIAL : FINE - GRAINED STEEL

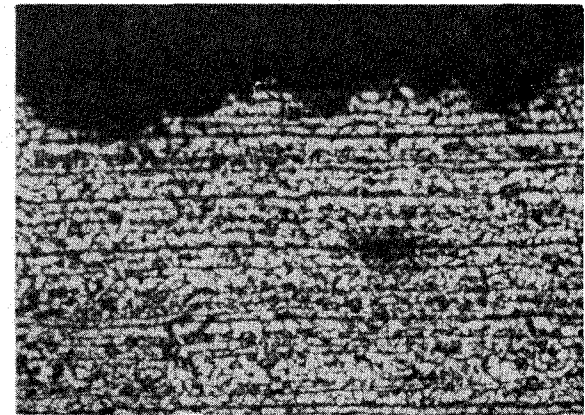
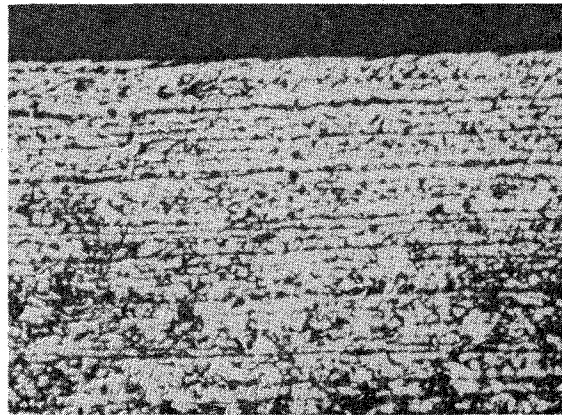
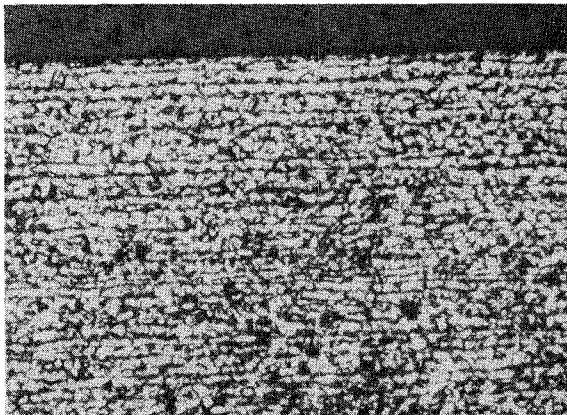
Before Exposure

After Exposure
without Gamma-Irradiation

T = 150°C, t = 900 d

After Exposure
with Gamma-Irradiation

T=150°C, t=700 d, \dot{D} ca. $3 \cdot 10^2$ Gy/h

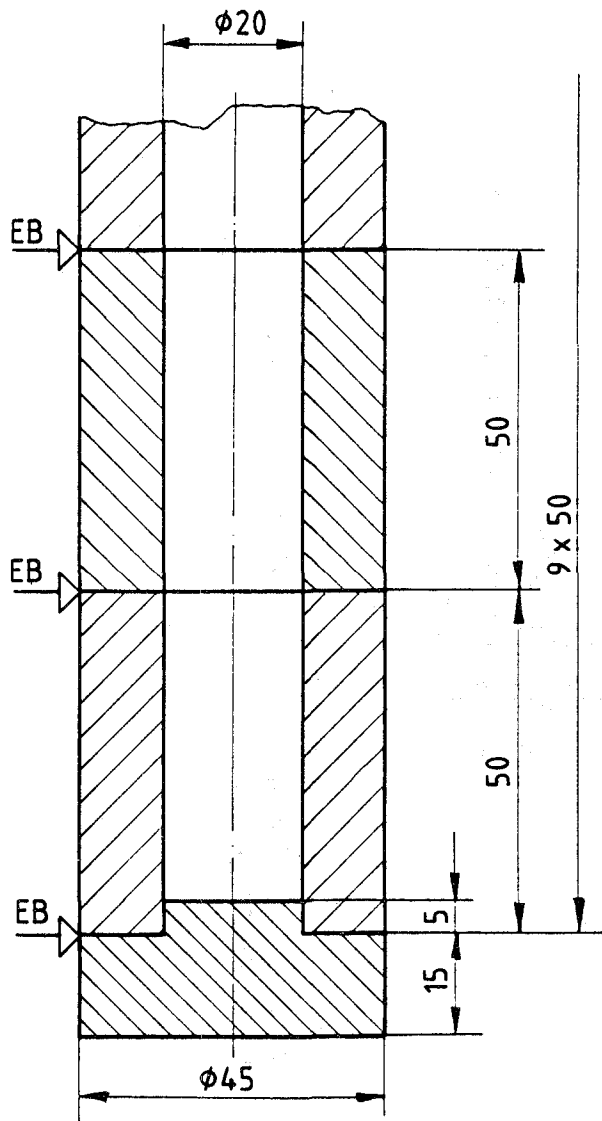


0.1 mm

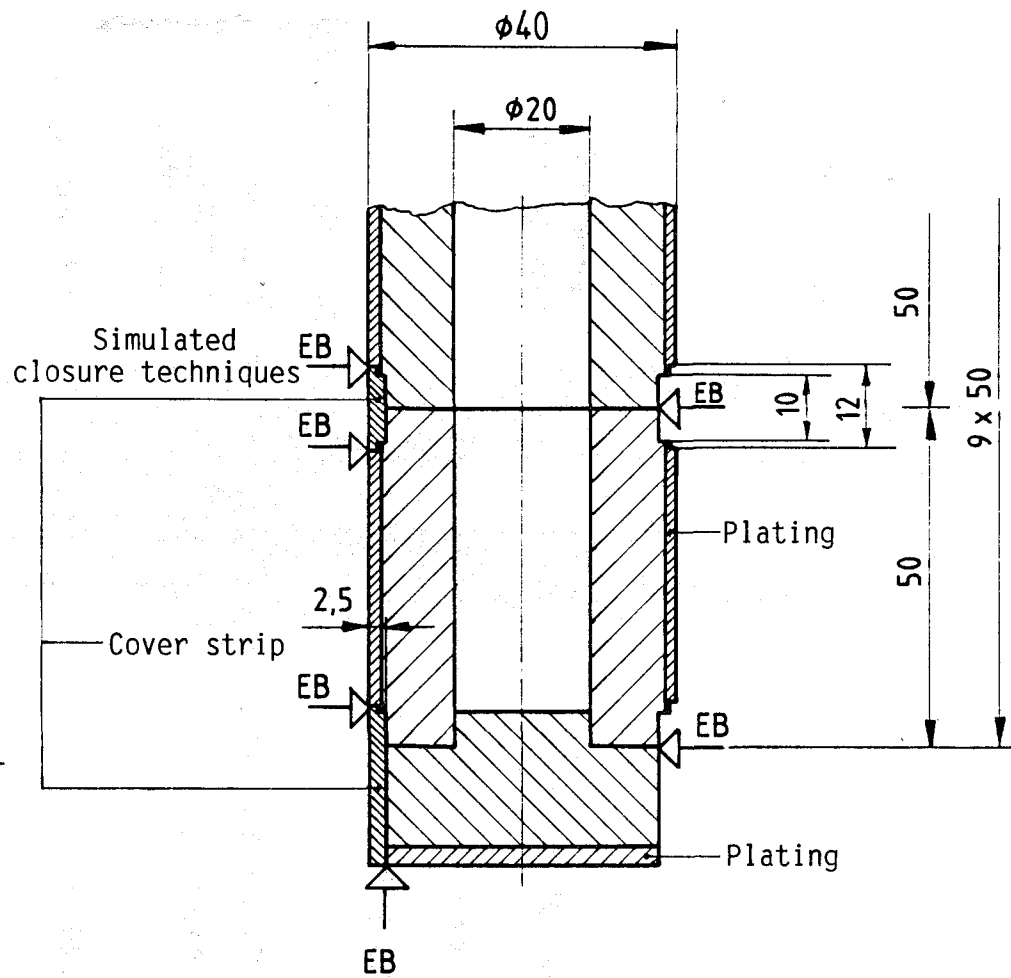
0.1 mm

0.1 mm

Fig. 16 Optical micrographs of fine-grained steel stored in the Brine Migration Test



Tube type I: cast steel GS 16 Mn5.



Tube type II: Ti 99.8-Pd plated
Hastelloy C4 plated

Fig. 17 Layout of in-situ tested cast-steel tubes with and without corrosion protection

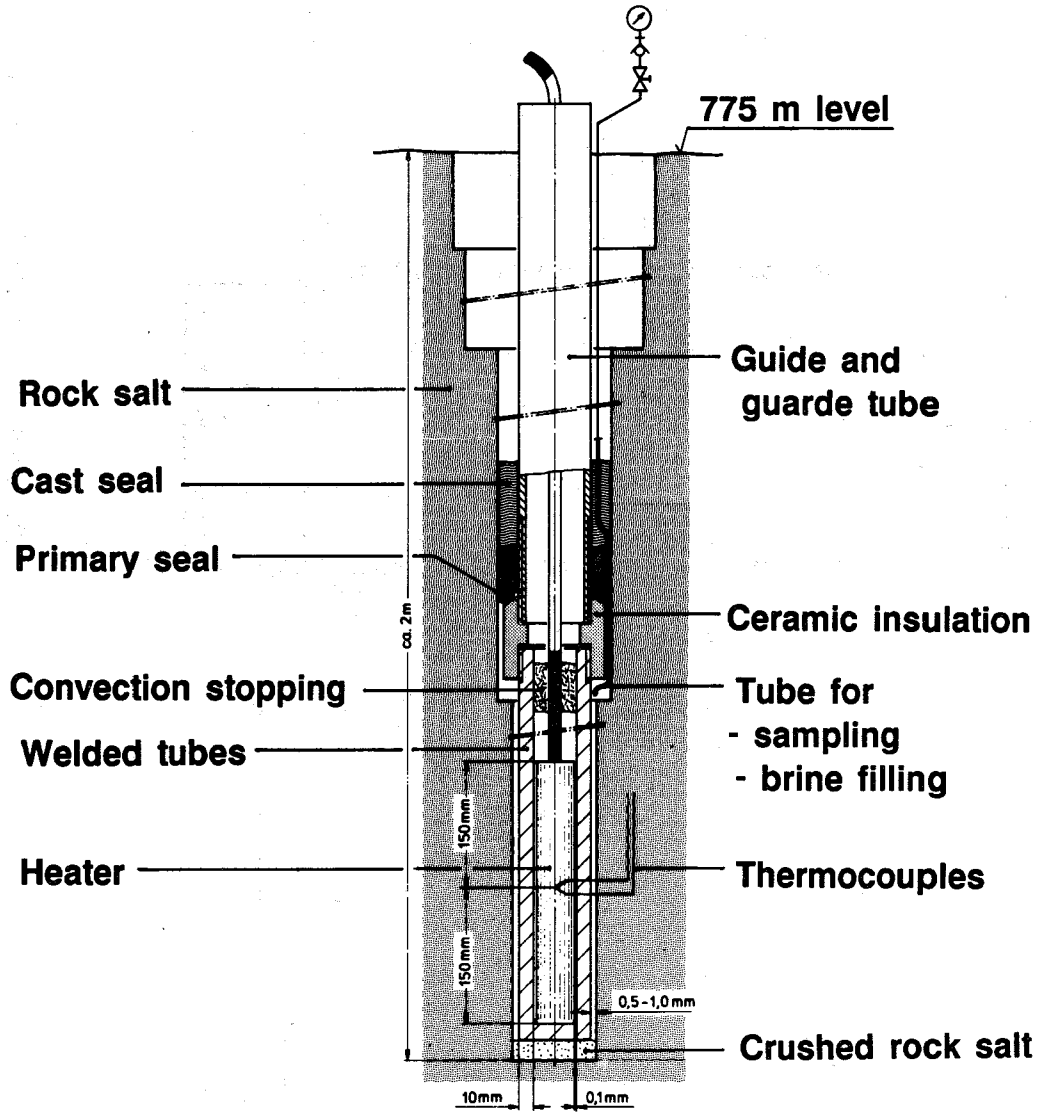


Fig. 18 Vertical section of test assembly for corrosion experiments on tubes

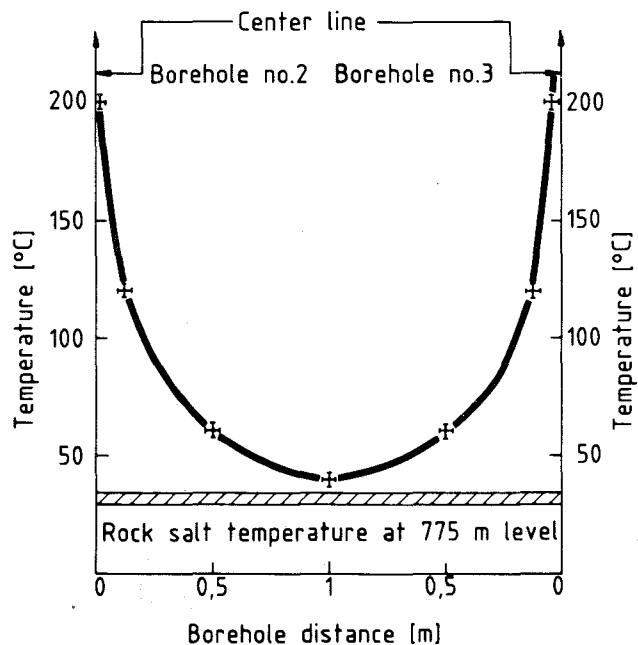


Fig. 19 Radial temperature distribution between two boreholes in the center of heated zone (in-situ corrosion experiments on tubes)

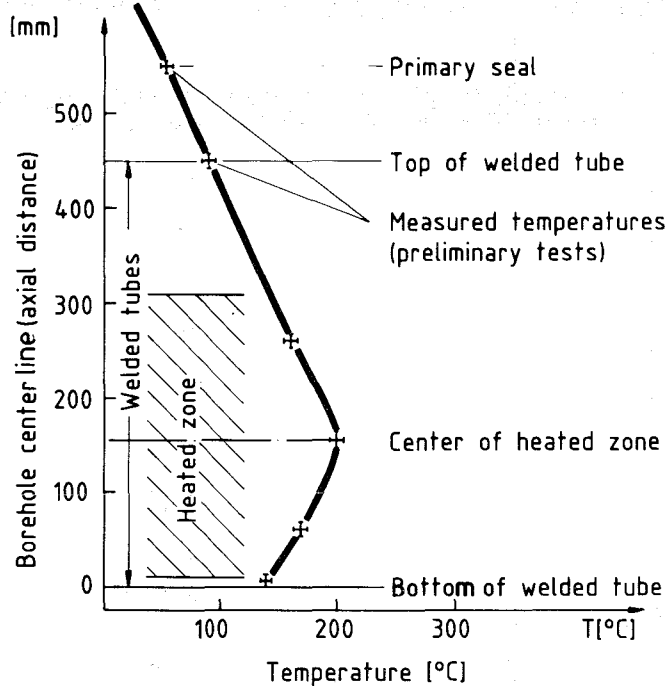


Fig. 20 Vertical temperature distribution on the wall of the tubes

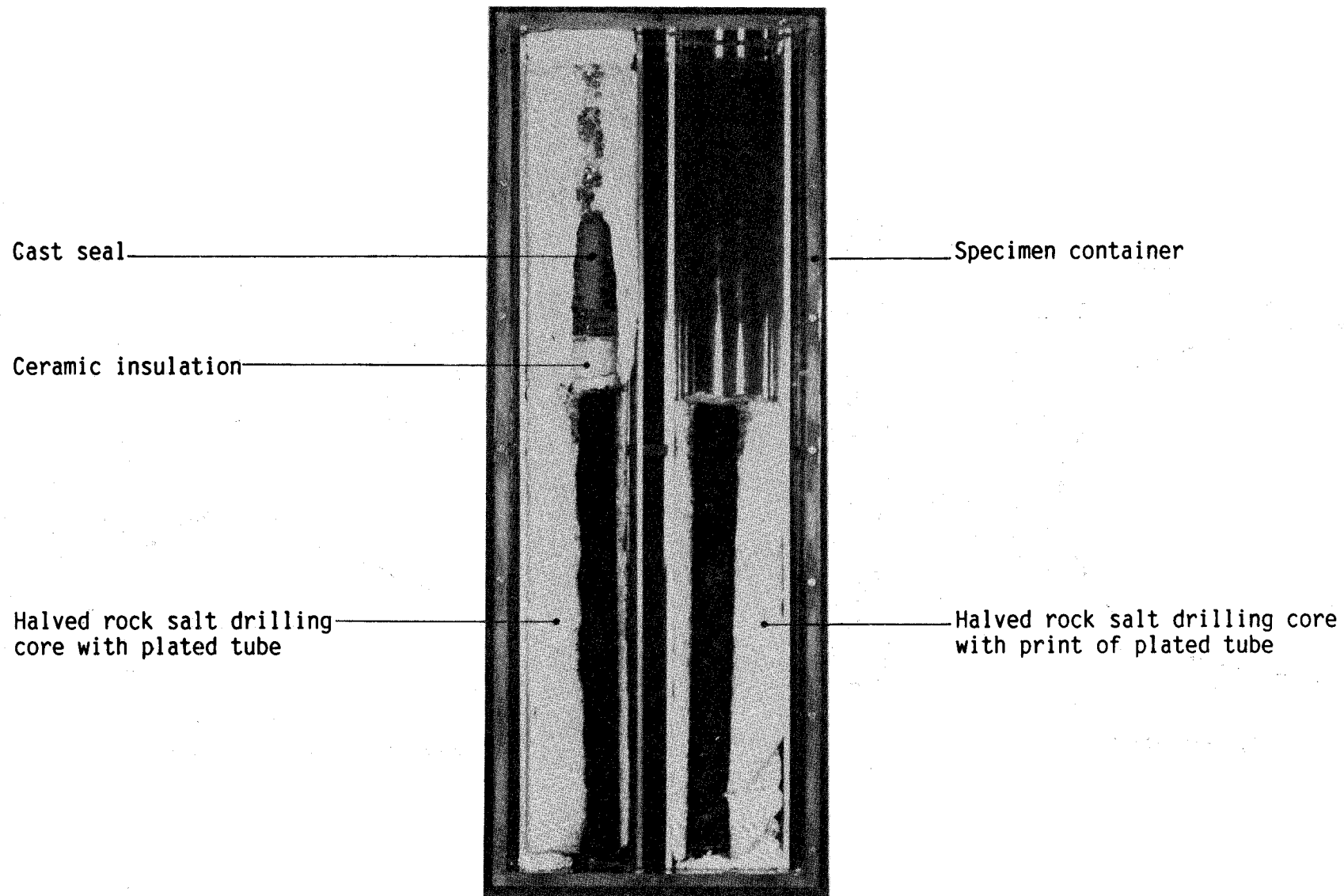
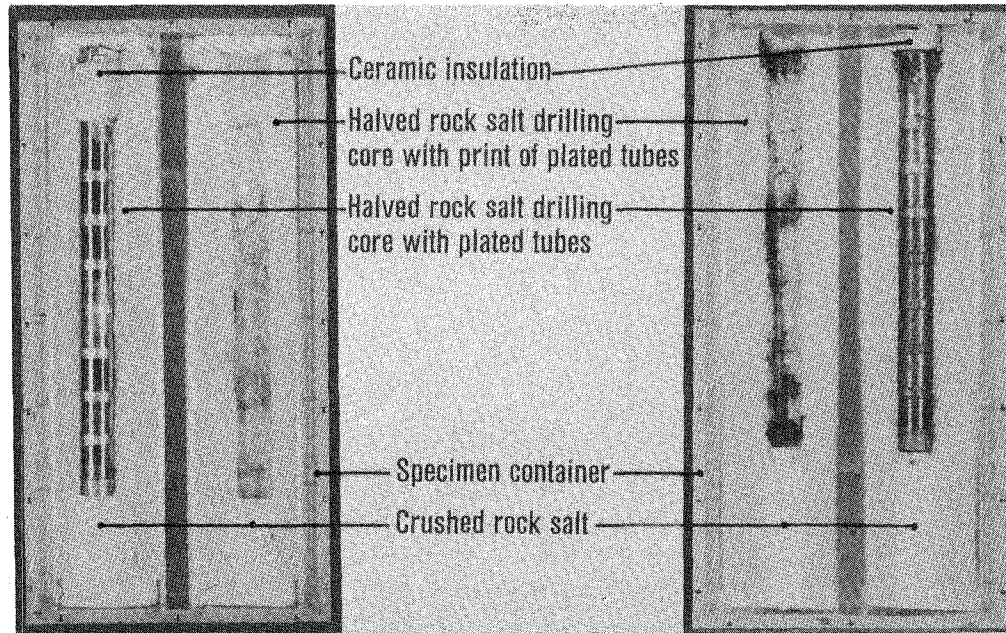


Fig. 21 Retrieved cast-steel tube after in-situ storage
(1.5 a in rock salt + 100 ml added NaCl brine at 90°C-200°C)



Explosion plated and EB welded corrosion protection

Hastelloy C4

Ti 99.8-Pd

Fig. 22 Retrieved cast-steel tube with corrosion protection after in-situ storage (1.5 a in rock salt + 100 ml added NaCl brine at 90°C-200°C)

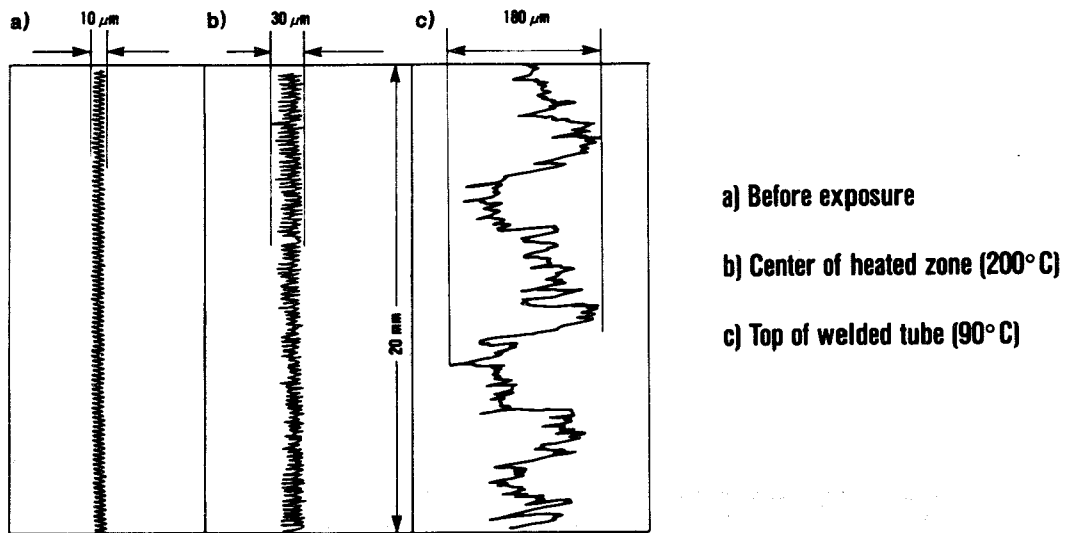


Fig. 23 Surface profiles of the cast-steel tube before and after 1.5 a in-situ storage in rock salt plus NaCl brine

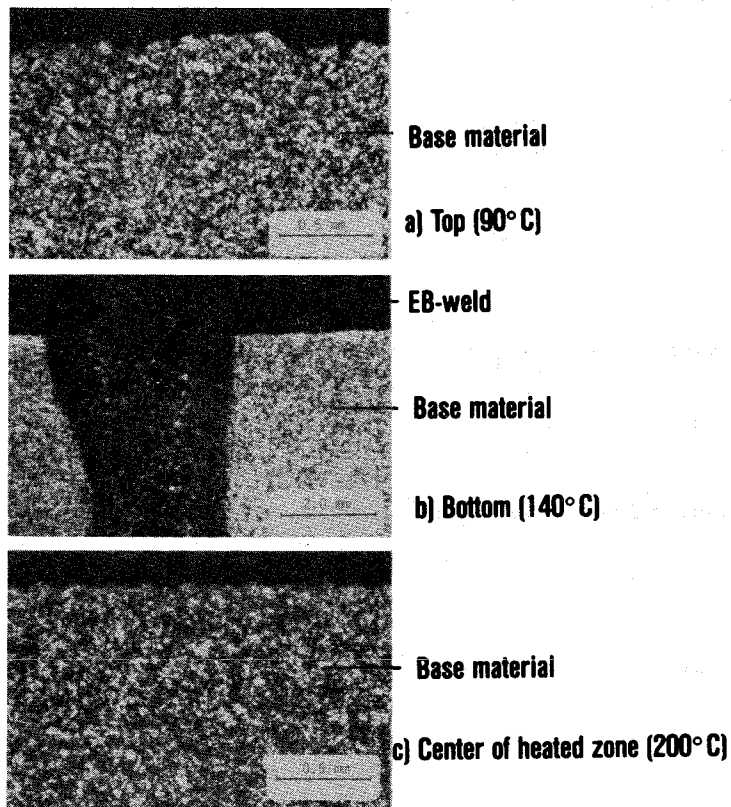
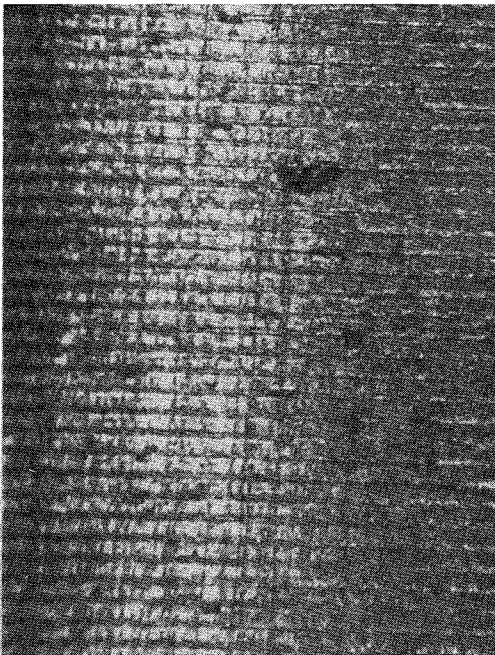
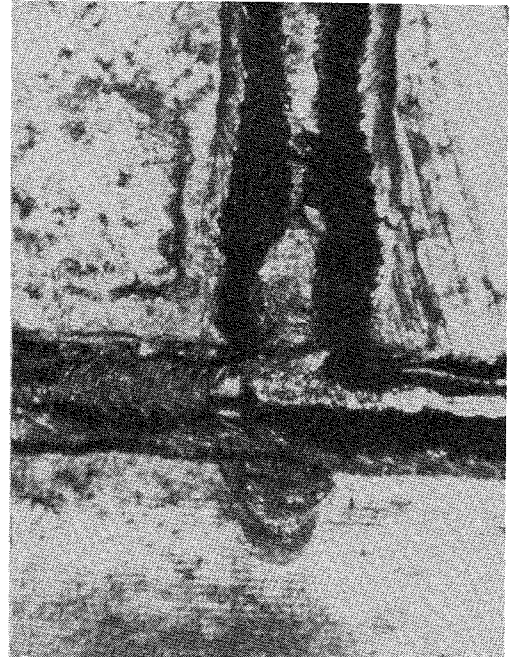


Fig. 24 Optical micrographs of cast-steel tube from different temperature zones after 1.5 a in-situ storage in rock salt plus NaCl brine

Details of manufacture



Mechanically finished surface turning

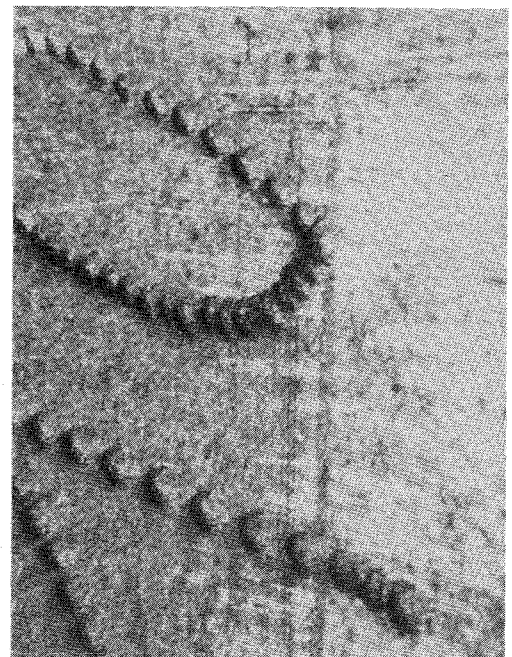


Weld and hot rolled sheet metal surface

**Ti 99.8-Pd
x 25**



Surface nicking

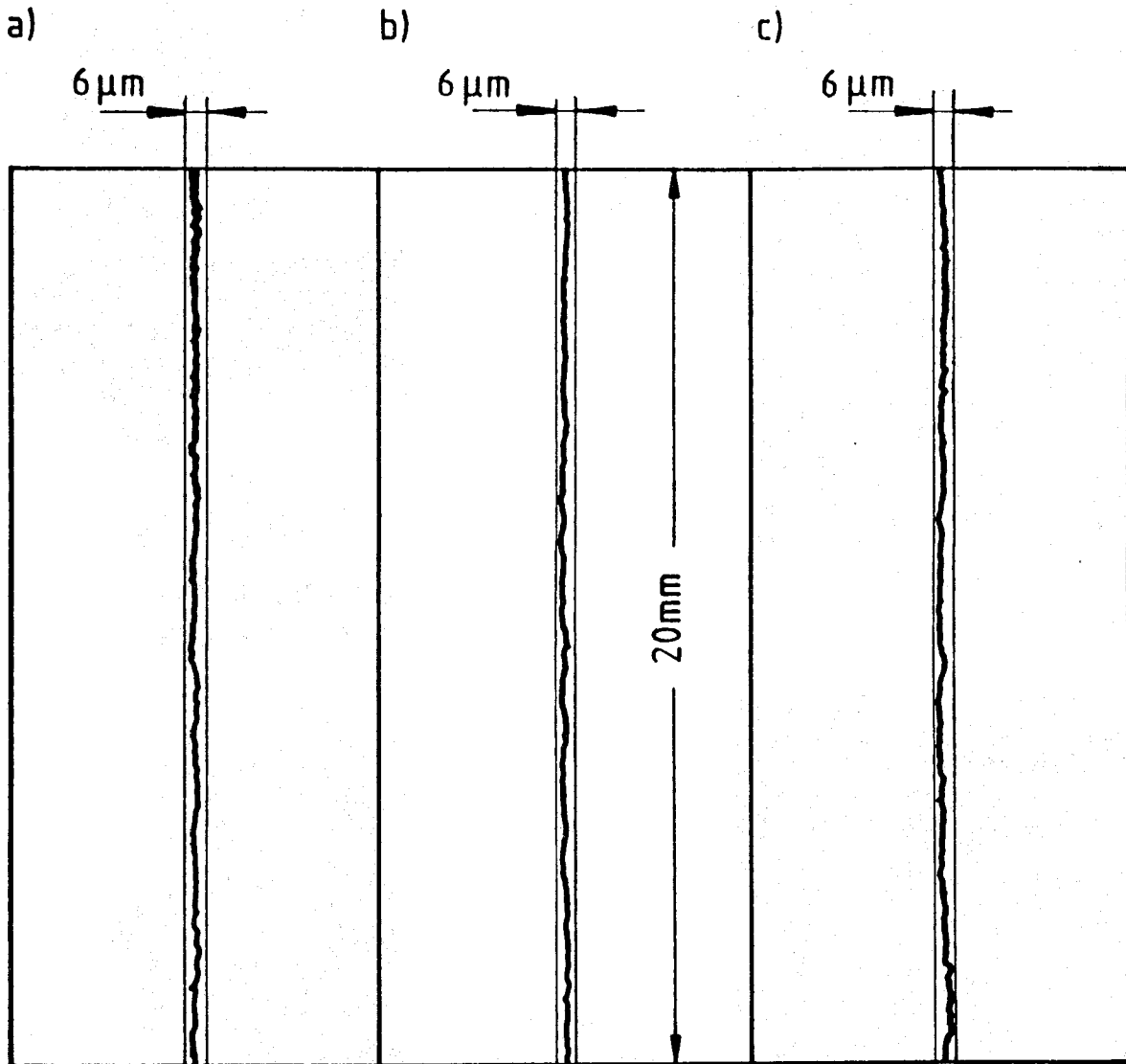


Crack produced by steel needle

Mechanical damage of surface

Electro-engraved figure

Fig. 25 Optical macrographs from the surface of the plated tube after 1.5 a in-situ testing in rock salt plus NaCl brine



a) Before exposure (Hastelloy C4 and Ti 99.8-Pd)

b) Center of heated zone (200°C , Hastelloy C4)

c) Top of welded tube (90°C , Ti 99.8-Pd)

Fig. 26 Surface profiles of the plated tubes before and after 1.5 a in-situ storage in rock salt plus NaCl brine

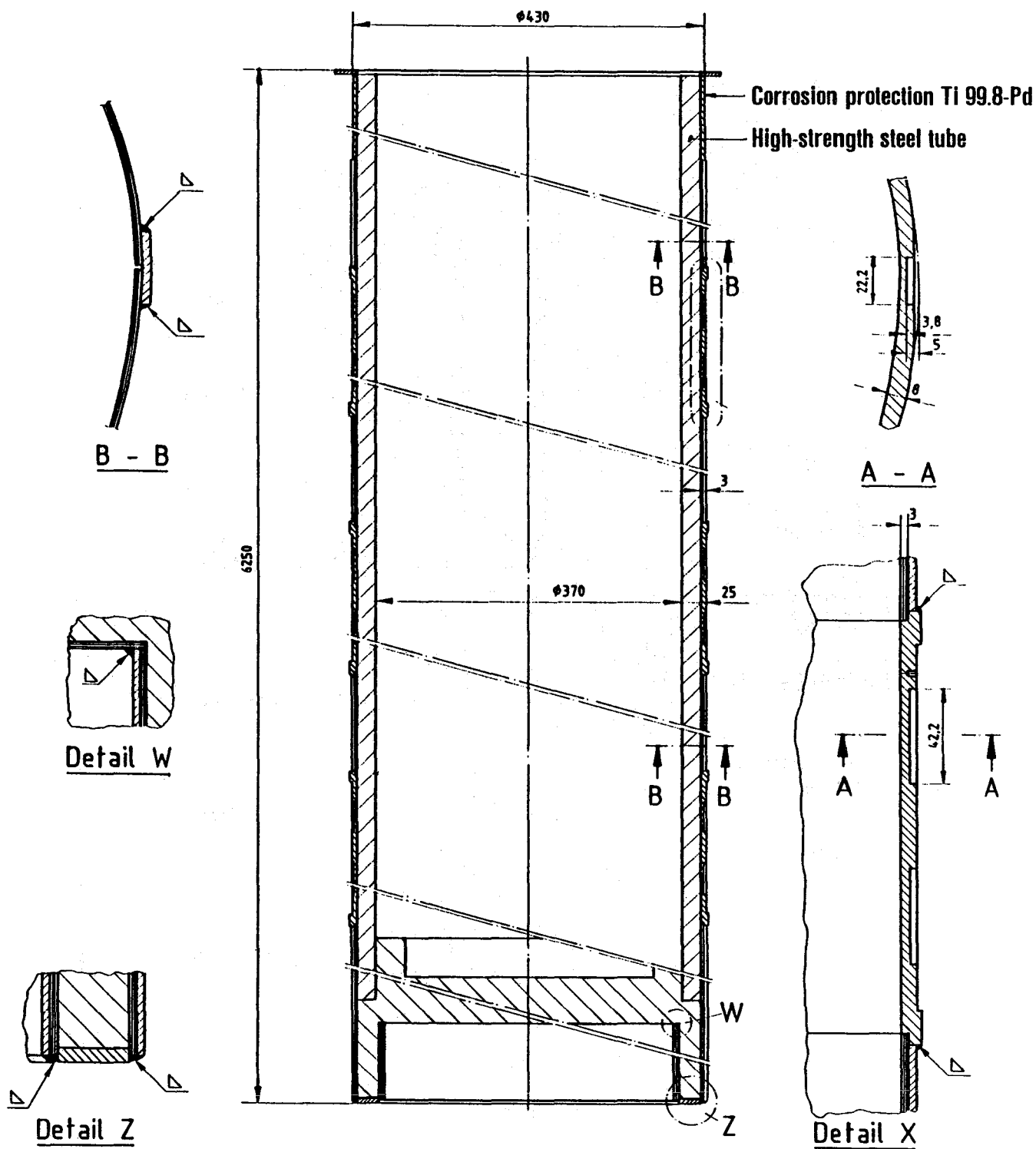


Fig. 27 Characteristics of the borehole casing for the HLW test disposal

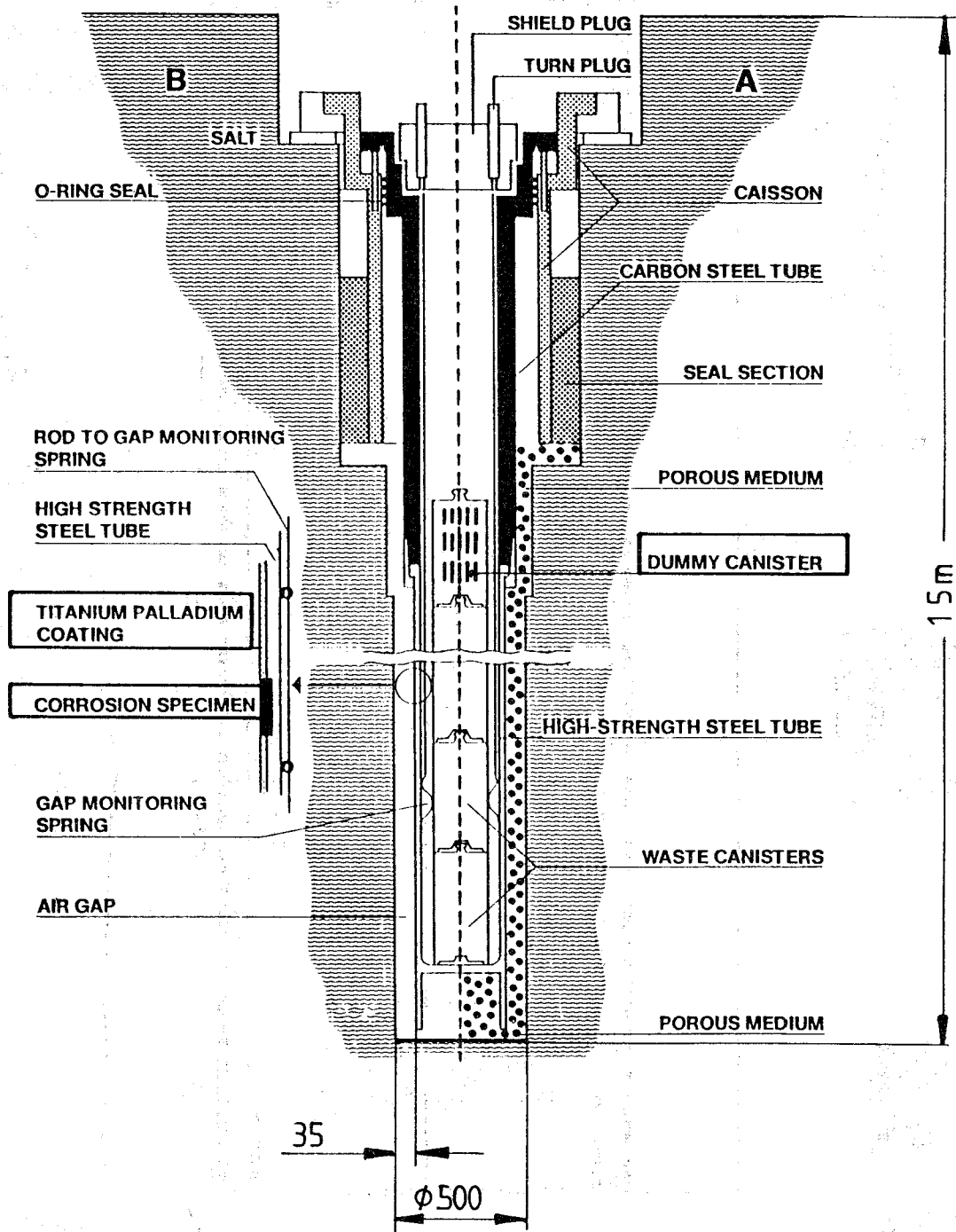


Fig. 28 Vertical section of test assembly for the HLW test disposal with indication of the specimens location

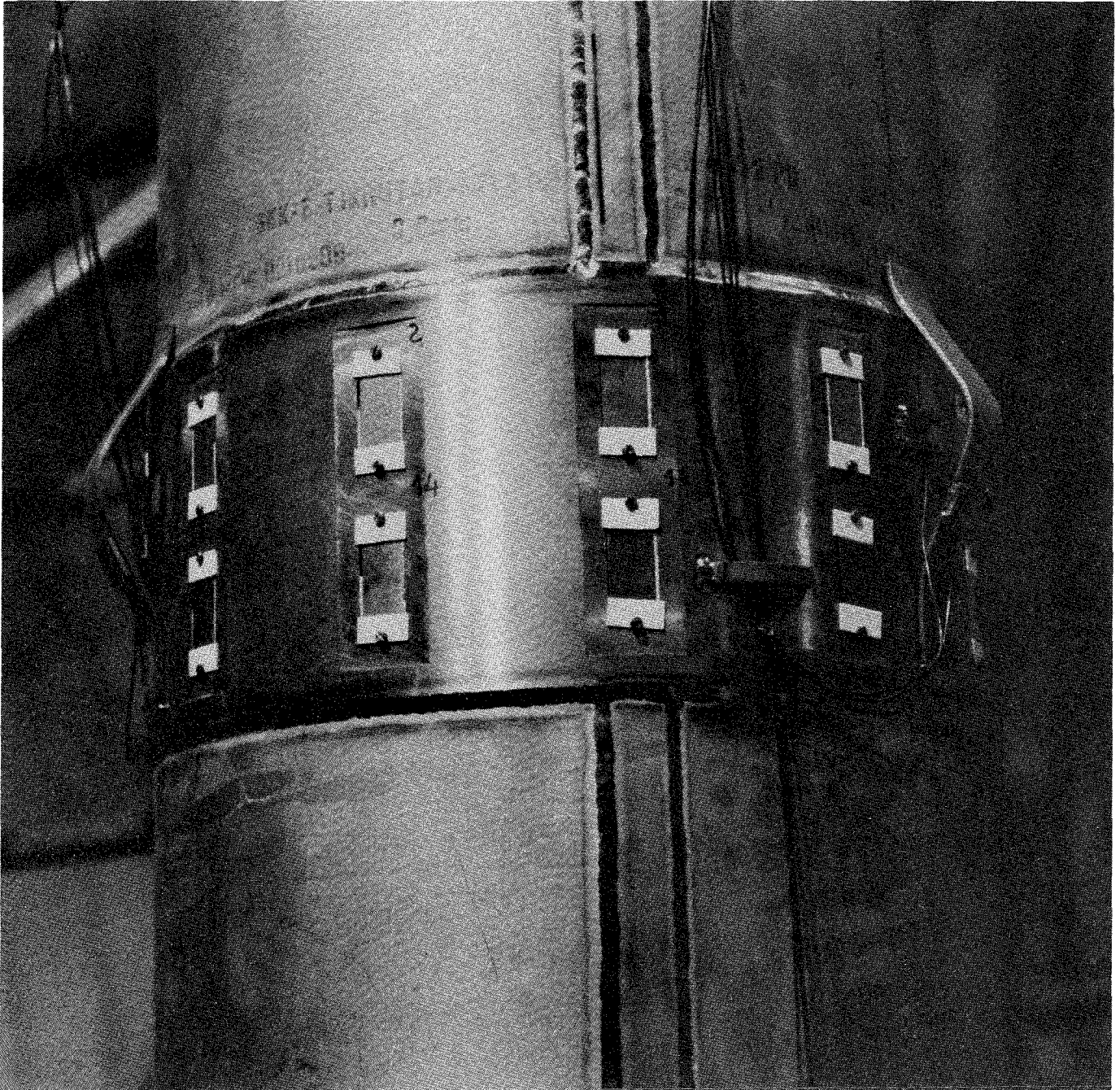


Fig. 29 Fixation of the corrosion specimens on the borehole casing before storage in the HLW test boreholes

Acknowledgements

The authors wish to thank Mr. T. Rothfuchs and the personnel of the Asse salt mine of the Gesellschaft für Strahlen- und Umweltforschung, Institut für Tieflagerung, Braunschweig, for discussions and support in carrying out the in-situ corrosion experiments.

This work has been supported by the Commission of the European Communities, Brussels, Belgium.